Atmosphere **2014**, *5*, 635-668; doi:10.3390/atmos5030635

OPEN ACCESS

atmosphere

ISSN 2073-4433

www.mdpi.com/journal/atmosphere

Article

A Survey of Mercury in Air and Precipitation across Canada: Patterns and Trends

Amanda S. Cole [1,*], Alexandra Steffen [1], Chris S. Eckley [2], Julie Narayan [1], Martin Pilote [3], Rob Tordon [4], Jennifer A. Graydon [5], Vincent L. St. Louis [5], Xiaohong Xu [6] and Brian A. Branfireun [7]

1 Air Quality Processes Research, Science & Technology Branch, Environment Canada, 4905 Dufferin St., Toronto, ON M3H 5T4, Canada; E-Mails: Alexandra.Steffen@ec.gc.ca (A.S.); Julie.Narayan@ec.gc.ca (J.N.)

2 U.S. Environmental Protection Agency, Region 10, 1200 6th Ave, Seattle, WA 98101, USA; E-Mail: Eckley.Chris@epa.gov

3 Aquatic Contaminants Research Division, Environment Canada, 105 McGill, Montreal, QC H2Y 2E7, Canada; E-Mail: Martin.Pilote@ec.gc.ca

4 Environment Canada, 45 Alderney Drive, Dartmouth, NS B2Y 2N6, Canada; E-Mail: rob.tordon@ec.gc.ca

5 Department of Biological Sciences, University of Alberta, Edmonton, AB T6G 2E9, Canada; E-Mails: jgraydon@ualberta.ca (J.A.G.); vince.stlouis@ualberta.ca (V.L.S.L.)

6 Department of Civil and Environmental Engineering, University of Windsor, 401 Sunset Ave., Windsor, ON N9B 3P4, Canada; E-Mail: xxu@uwindsor.ca

7 Department of Biology and Centre for Environment and Sustainability, University of Western Ontario, 1151 Richmond Street, London, ON N6A 5B7, Canada; E-Mail: bbranfir@uwo.ca

* Author to whom correspondence should be addressed; E-Mail: amanda.cole@ec.gc.ca; Tel.: +1-416-514-2652.

Received: 27 June 2014; in revised form: 21 August 2014 / Accepted: 26 August 2014 / Published: 11 September 2014

Abstract: Atmospheric mercury (Hg) measurements from across Canada were compiled and analysed as part of a national Hg science assessment. Here we update long-term trends of Hg in air and precipitation, and present more extensive measurements on patterns and trends in speciated Hg species (gaseous elemental mercury—GEM, reactive gaseous mercury—RGM, and total particulate mercury on particles <2.5 μm—$TPM_{2.5}$) at several sites. A spatial analysis across Canada revealed higher air concentrations and wet

deposition of Hg in the vicinity of local and regional emission sources, and lower air concentrations of Hg at mid-latitude maritime sites compared to continental sites. Diel and seasonal patterns in atmospheric GEM, RGM and $TPM_{2.5}$ concentrations reflected differences in patterns of anthropogenic emissions, photo-induced surface emissions, chemistry, deposition and mixing. Concentrations of GEM decreased at rates ranging from −0.9% to −3.3% per year at all sites where measurements began in the 1990s. Concentrations of total Hg in precipitation declined up to 3.7% yr^{-1}. Trends in RGM and $TPM_{2.5}$ were less clear due to shorter measurement periods and low concentrations, however, in spring at the high Arctic site (Alert) when RGM and $TPM_{2.5}$ concentrations were high, concentrations of both increased by 7%–10% per year.

Keywords: elemental mercury; total gaseous mercury; reactive mercury; gaseous oxidized mercury; particulate mercury; cycling of atmospheric mercury; mercury in precipitation; mercury trends

1. Introduction

Mercury (Hg) is a pollutant of concern due to its health effects and elevated concentrations in aquatic food webs. Current and historical anthropogenic activities have mobilized Hg from stable mineral deposits to the atmosphere, oceans, soils and biota. The atmosphere transports Hg around the globe and deposits it to vegetation, soils and water, where under certain conditions it can be methylated to toxic, bio-accumulative methylmercury [1]. In the atmosphere, gaseous elemental mercury (GEM) dominates due to its estimated 6–12 month lifetime in the atmosphere [2–4]; shorter-lived reactive gaseous mercury (RGM) and total particulate mercury (TPM) in the atmosphere can either be emitted directly or created by oxidation of GEM and taken up on particles, depositing within hours to weeks [5]. Conversion of Hg between these three inorganic forms can take place on various timescales and media and influence deposition and surface emissions. As a result, levels of Hg in air and precipitation across Canada can vary on timescales from hours to decades. Short-term temporal changes in atmospheric concentrations of Hg, such as diel and seasonal patterns, arise from changes in meteorology (e.g., temperature, winds, sunlight, precipitation) that lead to changes in emissions, mixing, chemistry and deposition. Therefore, these patterns may yield information about the chemistry and air-surface exchange of Hg at a particular location, whereas long-term trends are reflective of multi-year changes in the Hg budget on local, regional and global scales [6].

Environment Canada's Canadian Atmospheric Mercury Measurement Network (CAMNet) operated between 7 and 14 sites across Canada measuring total gaseous mercury (TGM, the sum of GEM and RGM) from 1994 to 2007. Some of these sites, which are predominantly rural or remote, are currently operated under the Canadian Air and Precipitation Monitoring Network (CAPMoN). From 2002 onward, selected CAMNet sites began making measurements of speciated Hg (GEM, RGM and $TPM_{2.5}$). Canada has also had up to 18 precipitation monitoring sites, in conjunction with the U.S.-led

Mercury Deposition Network (MDN), measuring total Hg in precipitation at some locations since 1996. Figure 1 shows the locations of all active and inactive sites across Canada where the data presented in this study were collected. While the map shows more than 30 sites widely spread across the country, measurements at some locations were collected for only a few months, as summarized in Tables 1–3, and not all sites made both air and precipitation measurements.

Here, concentrations of Hg in the atmosphere and in precipitation are profiled across Canada. The atmospheric data are reported as TGM when measured by a Tekran 2537 instrument alone, and GEM, RGM and $TPM_{2.5}$ when using the Tekran 2537/1130/1135 system. These data incorporate and update previous measurements reported for some sites [7–22] and include speciated Hg measurements at several newer sites for the first time. The data were collected and analyzed as part of a Canadian mercury science assessment [23]. Diel (Section 2.2) and seasonal (Section 2.3) patterns in atmospheric concentrations and precipitation fluxes, plus long-term trends at sites where Hg has been measured for several years (Section 2.4), are presented. Data collection and analysis methods are detailed in Section 3.

Table 1. Stations measuring total gaseous mercury (TGM) in Canada and mean daily concentrations over the entire measurement period.

Station	Network	Longitude (°W)	Latitude (°N)	Measurement Period for Data Included Here	Mean TGM ± SD ($ng \cdot m^{-3}$)
Little Fox Lake YK	NCP [a]	135.63	61.35	June 2007–November 2011	1.28 ± 0.17
Reifel Island BC	CAMNet	123.17	49.10	March 1999–Febuary 2004	1.67 ± 0.19
Saturna BC	CAPMoN	123.13	48.78	March 2009–December 2010	1.43 ± 0.20
Whistler BC	INCATPA [b]/CARA [c]	122.93	50.07	August 2008–November 2011	1.21 ± 0.20
Meadows AB	None	114.64	53.53	May 2005–December 2008	1.51 ± 0.21
Genesee AB	None	114.20	53.30	March 2004–December 2010	1.53 ± 0.25
Fort Chipewyan AB	CAMNet	111.12	58.78	June 2000–July 2001	1.36 ± 0.15
Esther AB	CAMNet	110.20	51.67	June 1998–April 2001	1.65 ± 0.15
Bratt's Lake SK	CAPMoN	104.71	50.20	May 2001–December 2010	1.44 ± 0.25
Flin Flon MB	CARA [c]	101.88	54.77	July 2008–June 2011	3.75 ± 2.22
Windsor ON	None	83.01	42.18	January 2007–December 2008	1.93 ± 0.80
Burnt Island ON	CAMNet	82.95	45.81	May 1998–December 2007	1.55 ± 0.22
Egbert ON	CAMNet	79.78	44.23	December 1996–December 2010	1.58 ± 0.29
Buoy ON	CAMNet	79.45	43.40	July–September 2005	1.71 ± 0.20
Kuujjuarapik PQ	CAMNet	77.73	55.30	August 1999–September 2009	1.68 ± 0.46
Point Petre ON	CAMNet	77.15	43.84	November 1996–December 2007	1.75 ± 0.33
St. Anicet PQ	CAMNet	74.28	45.12	August 1994–December 2009	1.60 ± 0.37
St. Andrews NB	CAMNet	67.08	45.09	January 1996–July 2007	1.38 ± 0.24
Kejimkujik NS	CAMNet	65.21	44.43	January 1996–December 2010	1.40 ± 0.31
Mingan PQ	CAMNet	64.17	50.27	January 1997–December 2000	1.57 ± 0.19
Southampton PE	CAMNet	62.58	46.39	January 2005–December 2006	1.23 ± 0.19
Alert NU	CAMNet	62.33	82.50	January 1995–December 2011	1.51 ± 0.37

[a] Northern Contaminants Program, Aboriginal Affairs and Northern Development Canada; [b] Intercontinental Atmospheric Transport of Anthropogenic Pollutants to the Arctic, Government of Canada Program for International Polar Year; [c] Clean Air Regulatory Agenda, Environment Canada.

Table 2. Stations measuring speciated mercury (GEM, RGM, and $TPM_{2.5}$) in Canada and mean values over the entire measurement period.

Station	Longitude (ºW)	Latitude (ºN)	Measurement Period for Data Included Here	Mean GEM ($ng \cdot m^{-3}$)	Mean RGM ($pg \cdot m^{-3}$)	Mean $TPM_{2.5}$ ($pg \cdot m^{-3}$)
Genesee AB	114.20	53.30	January–September 2009	1.40	5.0	4.5
Flin Flon MB	101.88	54.77	July 2010–May 2011	2.06	3.4	10.4
Churchill MB	94.07	58.75	March–August 2004	1.52	100.9	168.5
ELA ON	93.72	49.66	May 2005–December 2010	1.39	1.0	4.4
Mississauga ON	79.65	43.54	January–December 2009	1.40	3.7	6.5
Dorset ON	78.93	45.22	July 2008–March 2010	1.38	2.7	5.9
St Anicet PQ	74.28	45.12	January 2003–December 2010	1.52	3.0	17.5
Kejimkujik NS	65.21	44.43	January 2009–December 2010	1.34	0.5	4.2
Halifax NS	63.67	44.67	October 2009–December 2010	1.68	2.1	2.3
Alert NU	62.33	82.50	January 2002–December 2011	1.26	21.8	41.1

Table 3. Stations measuring Hg in precipitation in Canada and mean monthly concentration (volume-weighted means), precipitation, and deposition over the entire measurement period. MDN = Mercury Deposition Network; GSC = Geological Survey of Canada.

Station	Network	Long (ºW)	Lat (ºN)	Measurement Period for Data Presented Here	Mean Total Hg Conc. ($ng \cdot L^{-1}$)	Mean Monthly Precip (mm)	Mean Hg Dep. ($\mu g \cdot m^{-2} \cdot month^{-1}$)
Reifel Island BC	MDN	123.17	49.10	April 2000–Febuary 2004	5.6	68	0.38
Saturna BC	MDN	123.13	48.78	September 2009–January 2011	4.5	91	0.41
Fort Vermillion AB	GSC	116.02	58.38	December 2006–January 2008	4.3	22	0.10
Genesee AB	MDN	114.20	53.30	July 2006–December 2009	12.8	32	0.44
Crossfield AB	GSC	114.00	51.29	May 2006–December 2007	9.3	23	0.22
Henry Kroeger AB	MDN	110.83	51.42	October 2004–December 2009	11.7	25	0.35
Esther AB	MDN	110.20	51.67	April 2000–May 2001	14.2	14	0.21
Bratts Lake SK	MDN	104.72	50.20	June 2001–December 2009	11.2	26	0.37
Flin Flon MB	Edmonton	101.88	54.77	September 2009–December 2010	59.9	30	1.80
Churchill MB	GSC	94.07	58.75	June 2006–December 2007	5.3	15	0.11
ELA ON	MDN	93.72	49.66	November 2009–January 2011	9.6	69	0.77
Burnt Island ON	MDN	82.95	45.81	November 2001–March 2003	9.2	61	0.56
Egbert ON	MDN	79.78	44.23	March 2000–January 2010	8.4	57	0.47
Dorset ON	MDN	78.93	45.22	January 1997–December 1998	9.7	56	0.55
Point Petre ON	MDN	77.15	43.84	November 2001–March 2003	9.1	58	0.54
Chapais PQ	MDN	74.98	49.82	December 2009–January 2011	6.4	71	0.46
St. Anicet PQ	MDN	74.03	45.20	April 1998–August 2007	7.9	70	0.56
St. Andrews NB	MDN	67.08	45.08	July 1996–December 2003	6.6	86	0.56
Kejimkujik NS	MDN	65.21	44.43	July 1996–January 2010	5.2	111	0.58
Mingan PQ	MDN	64.23	50.27	April 1998–August 2007	5.0	77	0.39
Stephenville NL	MDN	58.57	48.56	Febuary 2010–January 2011	5.6	97	0.54
Cormak NL	MDN	57.38	49.32	May 2000–January 2010	4.2	94	0.40

Figure 1. Map of current and past Canadian Hg monitoring stations.

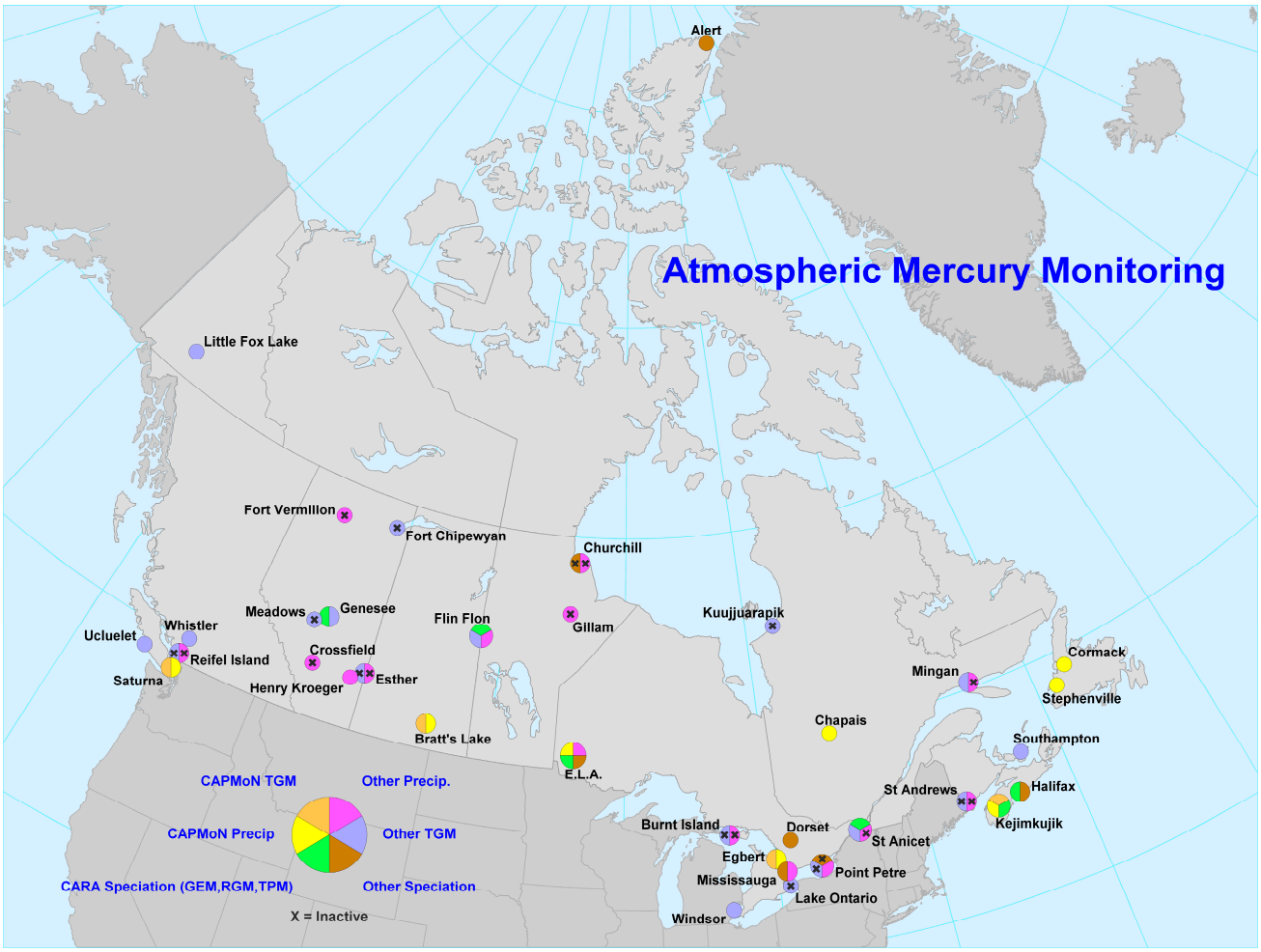

2. Results and Discussion

2.1. Spatial Patterns of Hg in Canada

The distribution of average daily TGM concentrations at 22 measurement sites is summarized by the box and whisker plot in Figure 2. Mean TGM concentrations at all but one of the sites ranged from 1.21 to 1.93 ng·m^{-3} (Table 1), within or below northern hemispheric background levels [24,25]. The bulk of TGM is GEM, with an atmospheric lifetime on the order of a year. Therefore, it is expected that TGM concentrations will be fairly uniform at background sites that are far from emission sources, except at sites where other atmospheric processes dominate [9]. The mean TGM concentration of 3.75 ng·m^{-3} observed at Flin Flon, MB, is a result of local emissions [19].

Overall, TGM concentrations and distributions at these Canadian sites are similar to previously reported data [8,9] where available, with small decreases at some sites observed over the long term (discussed further in Section 2.4). The sites with the lowest TGM levels, ranging from 1.21–1.38 ng·m^{-3}, include two high-elevation sites near the west coast (Whistler and Little Fox Lake) and three maritime sites at Southampton, Kejimkujik and St. Andrews. While the latter two sites began measurements in the 1990s, the other three cover more recent periods and the lower concentrations may be partially due to decreases in TGM since the 1990s [25,26]. The highest TGM levels by far

were observed at Flin Flon, due to local emissions from the copper smelter which was the largest point source of Hg in Canada before closure [19]. The sites that show the most variable TGM concentrations include Alert and Kuujjuarapik, which both experience episodes of rapid conversion of GEM to RGM and/or $TPM_{2.5}$ in the spring, known as atmospheric mercury depletion events (AMDEs) [27]. These AMDEs, as well as emissions from the snow and ocean in late spring and summer [28–31], lead to frequent and large fluctuations in TGM. Sites that were affected by local and regional pollution such as Windsor, Point Petre, Flin Flon and St. Anicet showed right-skewed distributions (*i.e.*, a long tail of higher concentrations) that were due to periodic episodes of high TGM concentrations. Similarly, the concentration data from the Lake Ontario Buoy, which is downwind of U.S. emission sources, and the Edmonton-area sites at Genesee and Meadows, which are downwind of local coal-fired power plants, also showed right-skewed distributions. TGM at Kuujjuarapik has a right-skewed distribution that is likely a result of the increased GEM concentrations in the spring and summer following the AMDE season. In contrast, TGM concentrations at Alert are left-skewed due to the periodic losses of GEM during AMDEs that have a greater effect on TGM levels in comparison to emissions. These seasonal cycles are discussed in more detail in Section 2.3.

Figure 2. A comparison of total gaseous mercury (TGM) measurements, west to east. The top section is compressed to include Flin Flon, MB. Time periods covered by measurements are listed in Table 1.

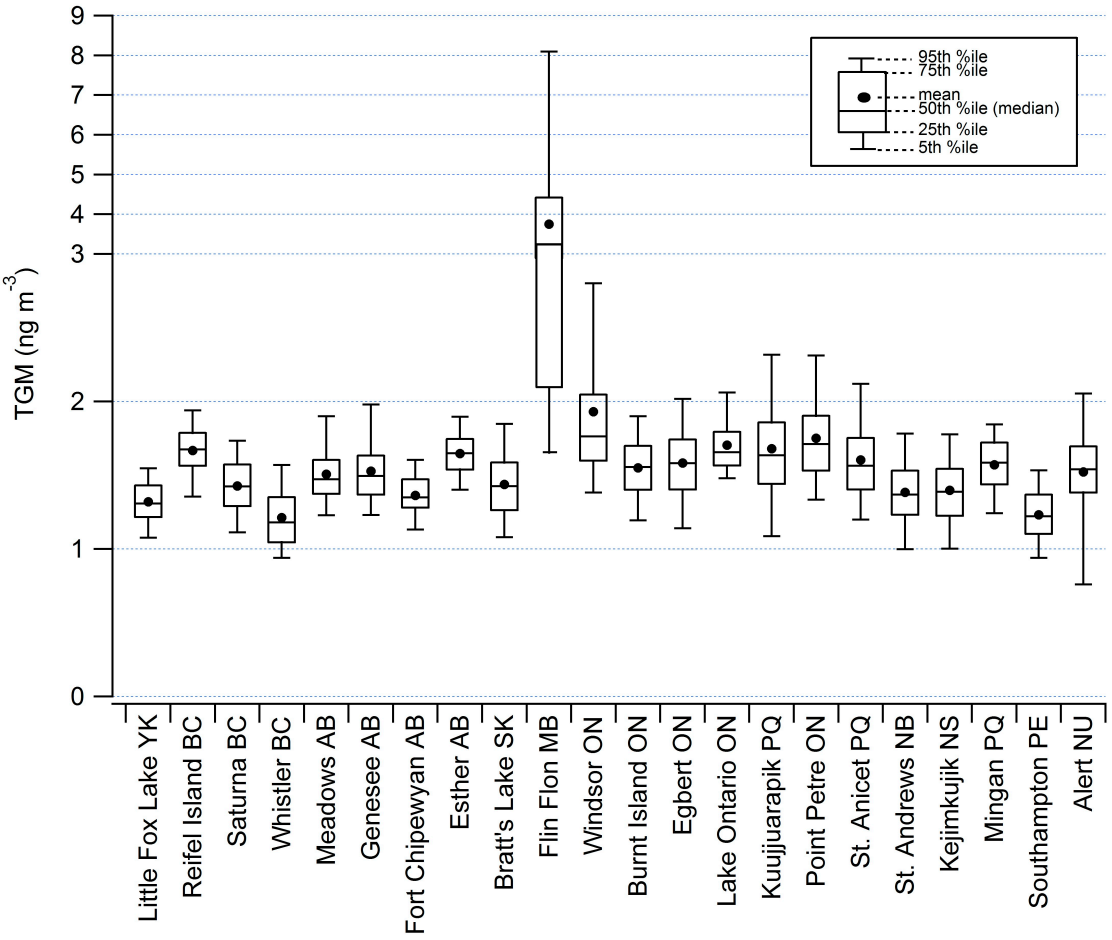

Measurements of RGM, $TPM_{2.5}$ and GEM at sites measuring atmospheric Hg speciation concentrations are summarized in Table 2. A box and whisker plot of RGM and $TPM_{2.5}$ is shown in Figure 3. At Alert and Churchill, the two sites bordering sea ice, RGM and $TPM_{2.5}$ levels spike in the spring due to AMDEs, when GEM is oxidized to RGM periodically [27]. While the highest RGM and $TPM_{2.5}$ concentrations were measured at Churchill, it should be noted that the Alert probability distribution represents data from several years and includes low RGM measurements from fall and winter. Data from Churchill were only collected for one spring and summer and therefore are more weighted by the spring months when RGM and $TPM_{2.5}$ values are high. Both sites have RGM and $TPM_{2.5}$ distributions highly skewed towards higher concentrations (mean >median), as expected of a site that is observing a local "source;" in this case, formation of RGM by local or regional chemistry [27,32].

Figure 3. Comparison of reactive gaseous mercury (RGM) and total particulate mercury ($TPM_{2.5}$) at mercury speciation stations. The top plot shows the full range to include Alert, NU, and Churchill, MB. Time periods covered by measurements are listed in Table 2.

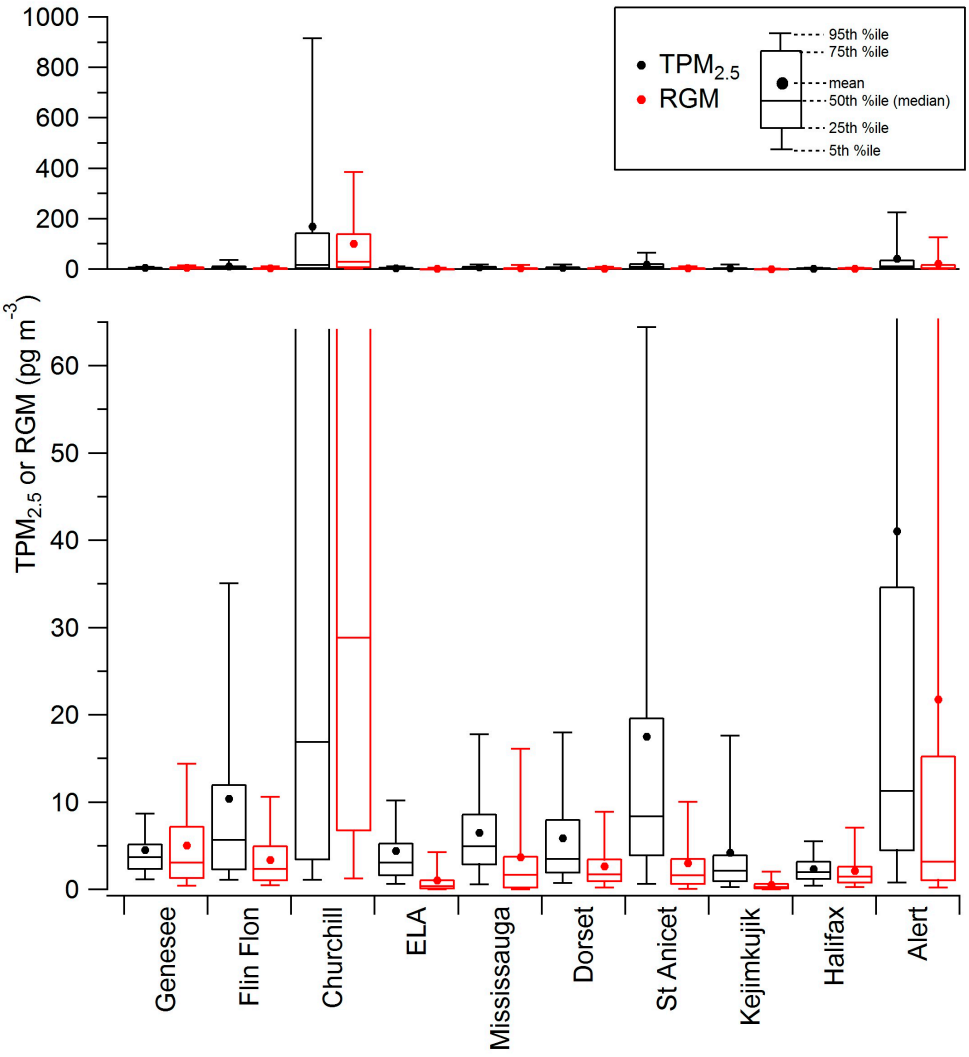

RGM is relatively short-lived with respect to deposition to particles or surfaces, with an estimated lifetime of a few hours to days [5]. Therefore, remote sites that are far from emission sources and are

not affected by AMDEs, such as the ELA and Kejimkujik, report very low concentration levels of RGM. In fact, the RGM concentration at these locations were below the manufacturer's suggested detection limit of ~2 pg·m^{-3} more than 75% of the time. Further, even some sites that would be expected to be affected by local emission sources (such as Mississauga, St. Anicet and Halifax) have median RGM levels below this detection limit (Figure 3), though method detection limits determined by blank measurements at individual sites may be lower (see Experimental section). Genesee and Flin Flon sites had higher RGM concentrations due to local sources of Hg pollution (coal-fired power plants [17] and a copper smelter [19], respectively) but concentrations were not as high as those reported in the Arctic at Alert and Churchill. Concentrations of $TPM_{2.5}$ were usually, but not always, higher than RGM (Table 2; Figure 3) such that median values were above the 2 pg·m^{-3} threshold at most sites. Similar to RGM, mid-latitude sites had lower $TPM_{2.5}$ concentrations than the northern coastal sites, Alert and Churchill. Concentrations of RGM and $TPM_{2.5}$ at mid-latitude sites were comparable to those reported by Gay *et al.* [18] for remote sites across the United States, plus Kejimkujik, for 2009–2011.

Speciated Hg was measured at Flin Flon starting in July 2010, a few weeks after the shutdown of the copper smelter. Concentrations of RGM and $TPM_{2.5}$ were elevated above background levels (represented at the ELA site), likely due to residual effects from the smelter activities, and were similar to concentrations at other rural sites affected by regional pollution sources, such as St. Anicet and Genesee (Figure 3). The mean TGM concentration measured with the speciation system SSW of the smelter is higher than at other sites at 1.91 ng·m^{-3} but lower than measured at the TGM-only site SSE of the smelter during the same period (3.17 ng·m^{-3}), likely because it is usually upwind of the source [19].

It should also be noted that since RGM and $TPM_{2.5}$ are operationally defined, comparisons between different sites are problematic. For example, the specific compounds that make up RGM may vary between sites, and if those compounds are retained by the denuder column with different efficiencies [33], some of what is RGM may be measured as GEM. In addition, ozone has been shown to decrease the collection efficiency of RGM on the denuder [34], which may suppress observed RGM levels at more polluted sites. Finally, $TPM_{2.5}$ measures only those particles smaller than 2.5 μm, so persistent differences in the size of aerosol at different sites (e.g., due to differences in humidity or the age of particles) would also affect the relative amounts of $TPM_{2.5}$ measured at those sites.

Monthly volume-weighted mean total Hg concentrations in precipitation and monthly Hg wet deposition rates are shown in Figure 4 and Table 3. The site locations for the atmospheric measurements differ from the wet deposition sites with only 13 in common for both types of sampling. The range of values for mean monthly deposition of Hg was 0.10–0.77 μg·m^{-2}·month^{-1}, or 1.2–9.2 μg·m^{-2}·yr^{-1}, excluding Flin Flon. These values are similar to or lower than what was found for MDN sites across North America outside of the southeastern US, where deposition rates for 2005 were on the order of 10–20 μg·m^{-2}·yr^{-1} [16]. As with TGM measurements, precipitation measurements at Flin Flon include time periods when the smelter was operational and thus the Hg deposition rates were 2–18 times higher than at other sites.

The lowest Hg wet deposition rates were observed at Fort Vermilion and Churchill, the most northerly of the precipitation monitoring sites, where concentrations of Hg in precipitation were also low. Sites with low precipitation volumes in Alberta and Saskatchewan had high concentrations of Hg

in precipitation but low overall deposition. Low precipitation amounts can lead to low wet deposition and high concentrations of Hg as both $TPM_{2.5}$ and RGM can build up in the air or on cloud droplets before being deposited in rain or snow. At this time, there are insufficient co-located speciation measurements to confirm this hypothesis. In contrast, sites near the west and east coasts, where total precipitation volumes were high, had low concentrations of Hg in precipitation (due to dilution) but higher wet deposition than the drier remote sites. Finally, with the exception of the ELA, sites closer to industrial activity in Ontario, Québec and the northeastern United States had relatively high concentrations of Hg in rain and snow (similar to the drier western sites) and the highest wet deposition amounts as a group. The ELA showed the highest average wet deposition of all the sites aside from Flin Flon, however, it should be noted that fewer than two years of data are presented here from the ELA and 10 other sites, and our ability to discern general spatial patterns from these data is therefore limited due to inter-annual variability. An earlier long-term study at the ELA reported a volume-weighted mean concentration of total Hg of 5.7 $ng \cdot L^{-1}$ for 1992–2006 [35] rather than the 11.2 $ng \cdot L^{-1}$ reported here.

Figure 4. Comparison of total Hg concentrations in precipitation (top) and monthly wet deposition (bottom), with only the mean shown for Flin Flon. Time periods covered by measurements are listed in Table 3. The distributions are based on monthly volume-weighted means and monthly deposition amounts, which were first calculated from weekly samples (see Experimental).

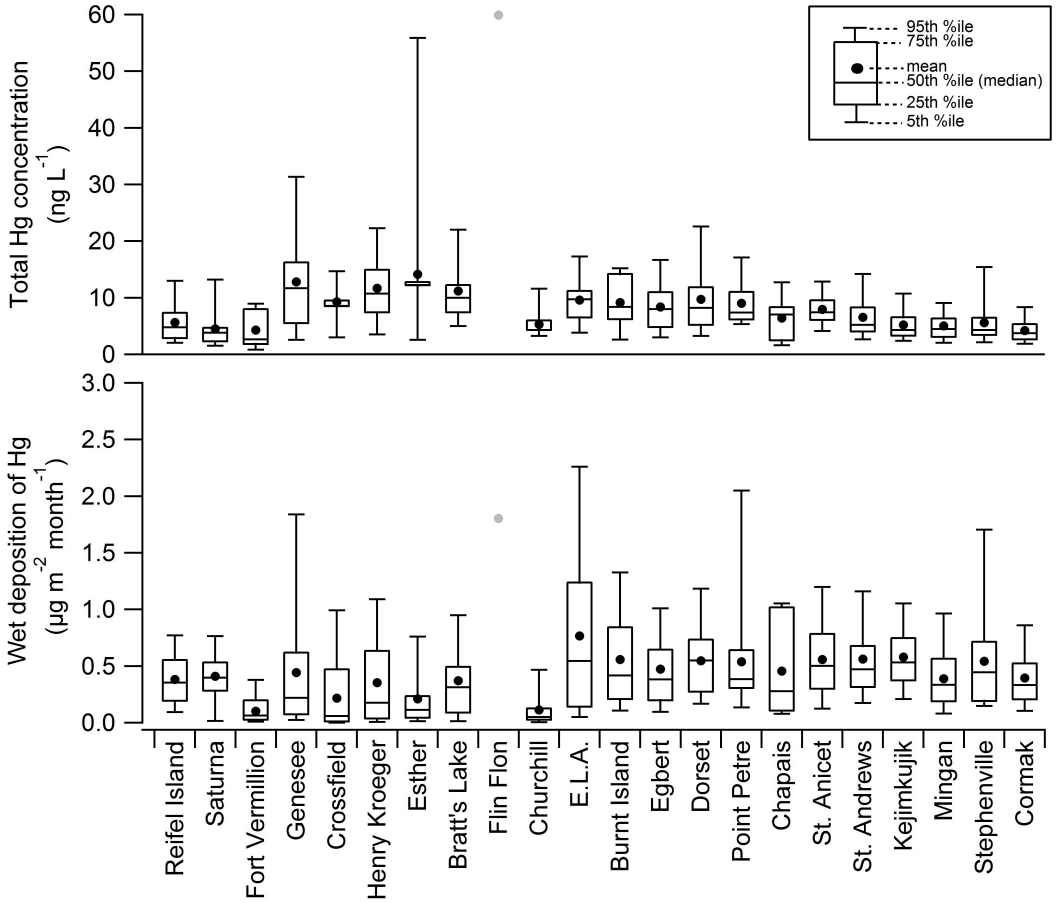

2.2. Diel Patterns of Atmospheric Hg

Plots of diel patterns in TGM are shown Figure 5. In this and all following figures, Alert is assigned to Atlantic Standard Time (UTC-4) since the maximum solar radiation occurs at noon in that time zone. Figure 5 shows that 14 of the 22 sites, as well as Flin Flon [19], have a similar daily pattern of a pre-dawn minimum and afternoon maximum. The afternoon peak is broad because data from all seasons have been averaged in the overall profile, and peaks can vary in timing and amplitude by season, with the strongest cycles observed in spring and summer. The diel patterns reported here are consistent with previous reports [8,10]. Kellerhals *et al.* [8] attributed this pattern to two factors: (1) night time deposition of TGM from the shallow nocturnal boundary layer followed by mixing with more TGM-rich air aloft when the nocturnal inversion breaks down; and (2) surface emission of TGM during the daytime following photolytic or temperature-driven processes on soils or snow [31,36–38]. This pattern has also been observed at other non-urban sites in North America (e.g., [e.g. 39,40]). The TGM diel cycle at St. Anicet is slightly different, with a second peak around 22:00. Previous analysis of St. Anicet data identified the influence of nighttime regional anthropogenic and industrial sources at this location [41].

At Alert, TGM concentrations were quite stable with a variation of about 0.05 ng·m^{-3} or 3%, likely because it is in constant light or darkness for most of the year [13]. TGM peaked around 11:00 but dropped quickly after noon, reaching a minimum around 20:00 and slowly increasing throughout the night and morning. This pattern was strongest in the springtime with an amplitude of 15% in April.

Figure 5. Diel cycles in TGM averaged over total measurement period at all sites. Hour 0 is from 12:00 to 1:00 a.m. local time.

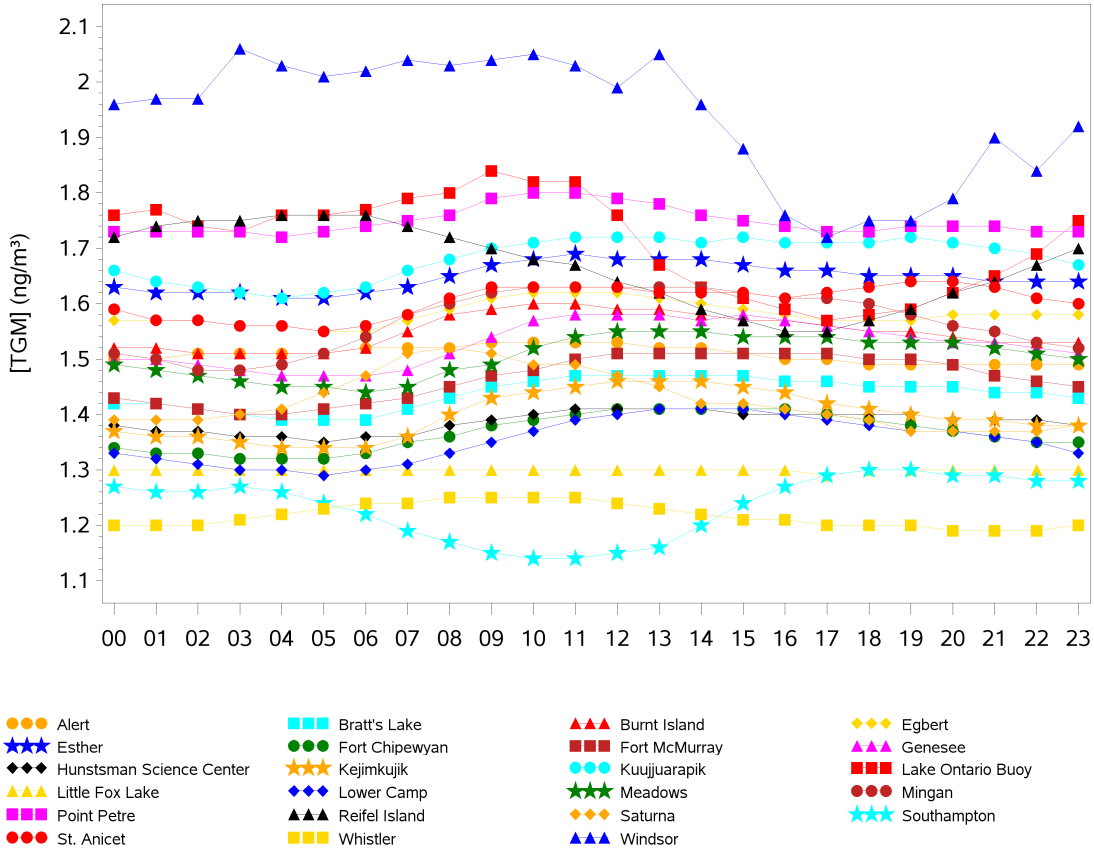

The remaining six sites had atypical diel patterns. TGM concentrations at Little Fox Lake did not vary with time of day, while Southampton was the only site with a late morning minimum. While no meteorological data was available for Southampton, the diel pattern of TGM was almost exactly opposite the diel pattern in wind speed at the nearby weather station at St. Peter's, 6 km to the northeast. At Reifel Island, Saturna and on the Lake Ontario Buoy, TGM concentrations peaked in the early, mid-, and late morning, respectively, then dropped through the afternoon to an evening minimum. Windsor also saw minimum TGM concentrations in the evening, rising to a broad peak between 03:00 and 13:00. This pattern at Reifel Island was previously attributed to changes in wind direction over the day, with daytime sea breezes bringing clean air from the ocean and nighttime land breeze transporting the TGM-rich plume from Greater Vancouver past the site [8]. The other three sites are also influenced by sea or lake breezes and are near to metropolitan areas. Urban areas in North America that report similar diel cycles in TGM or GEM include Detroit, MI, with maximum GEM at 05:00 and minimum around 15:00 [42] and Birmingham, AL, with maximum GEM around 10:00 and minimum around 16:00 [40]. It has been postulated that the decrease in urban GEM concentrations through the day to an afternoon minimum is due to the presence of high surface concentrations of Hg from local sources that are increasingly diluted by cleaner air from above as the day warms and vertical mixing is enhanced [40]. However, this pattern is not seen at all urban sites [e.g. 43] and it remains unclear what drives the diel patterns at these four Canadian sites.

Diel patterns of RGM, $TPM_{2.5}$ and GEM were also investigated for 10 different sites. These profiles are shown for every site except Flin Flon in Figure 6. RGM concentrations at all sites peaked in the afternoon, with amplitudes of 35%–180% of the mean. This suggests that short-lived RGM is formed through photo-oxidation of GEM in the atmosphere [44]. An afternoon maximum may also be due to higher RGM concentrations in the free troposphere (e.g., [45,46]) that mix down to the surface during the day. Higher concentrations aloft could arise from the slower nighttime dry deposition above the nocturnal boundary layer. These two mechanisms—*in situ* photo-oxidation and mixing with higher RGM levels above—could explain the consistent diel pattern across North American sites [39,40,42,43]. At certain sites, such as Genesee, local emission sources that release RGM above the nocturnal boundary layer, such that these releases are not mixed into the surface air until daytime [47], could contribute to the observed pattern as well.

The y-axis scales on both the Alert and Churchill plots in Figure 6 should be noted as the concentrations of RGM at these sites are significantly higher than at the others. This is a direct result of the springtime atmospheric chemistry that occurs at these locations. At Alert, the diel cycle of RGM is dominated by relatively large variability in the spring, when minimum and maximum concentrations can vary by up to 35 $pg \cdot m^{-3}$ (30% of the mean) with a broad peak in the afternoon. However, RGM concentrations vary widely at all times of day, and remain elevated throughout the night in the early spring when there is still a day/night cycle, suggesting that RGM has a lifetime of at least several hours, if not days, leading to elevated concentrations throughout the region. RGM levels at Alert could therefore be influenced by regionally elevated RGM and $TPM_{2.5}$ and depleted GEM [48], with an additional contribution from local photochemical production [32]. RGM concentrations at Churchill are similarly elevated throughout the day and night with a peak in the afternoon, again suggesting contributions from non-local as well as local chemistry.

Figure 6. Diel cycles in concentrations of GEM, RGM and $TPM_{2.5}$ (mean concentrations for each hour) at nine sites. Axis scales for RGM and $TPM_{2.5}$ vary.

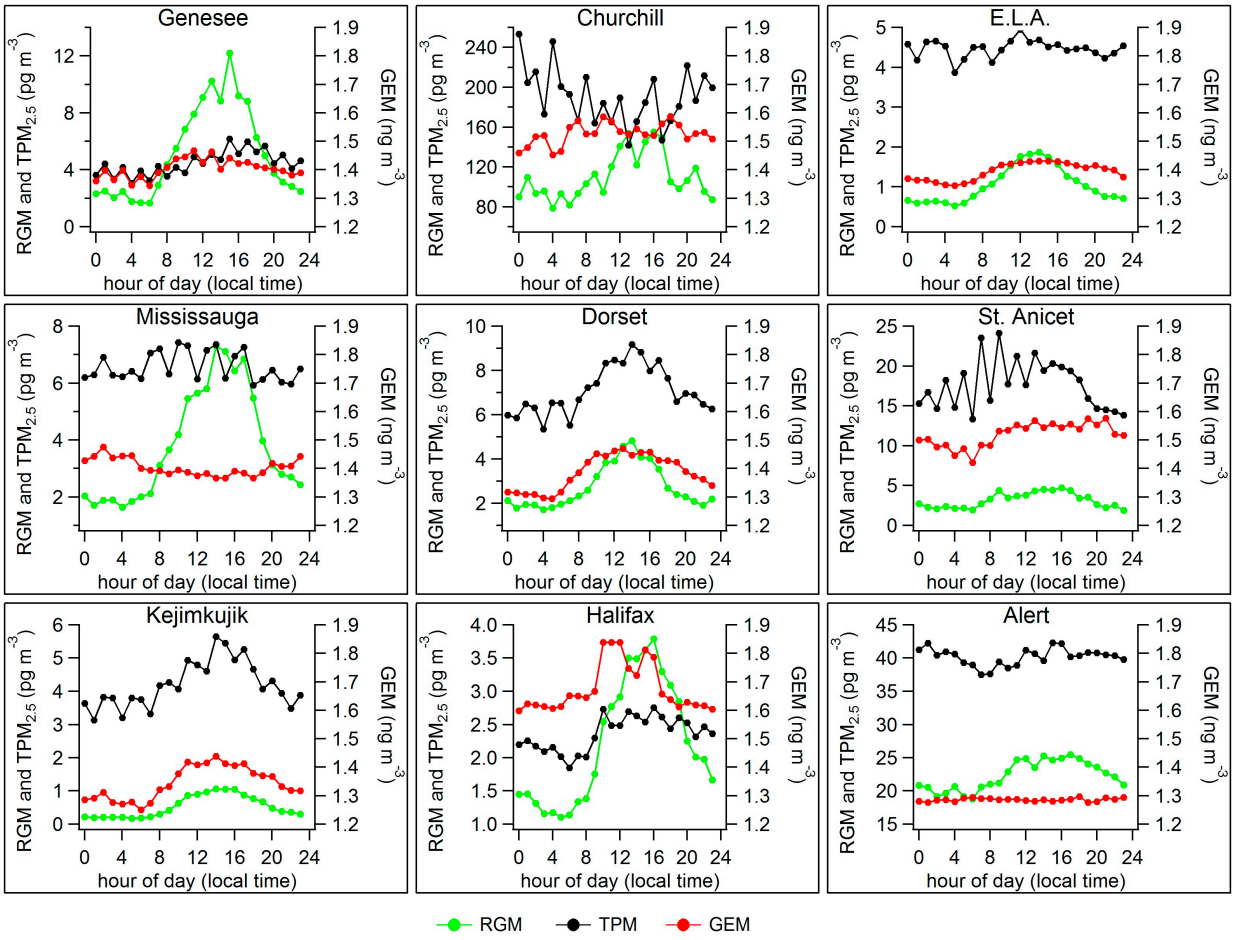

Diel patterns in $TPM_{2.5}$ concentrations are less consistent between sites than those observed for RGM. Particulate Hg is influenced by many factors, such as the amount of particulate available, the temperature (which can influence the partitioning between the gas and particle phases for semi-volatile compounds), transport of TPM from sources, and precipitation events that remove TPM from the air. At some sites, such as Dorset, St. Anicet, Kejimkujik and Genesee, $TPM_{2.5}$ is higher in the afternoon, though the time of maximum $TPM_{2.5}$ varies. At other sites such as ELA, Mississauga and Halifax, concentrations vary little across the day (<1 pg·m^{-3}). Only Churchill shows a minimum in $TPM_{2.5}$ levels during the daytime. $TPM_{2.5}$ patterns at other sites in North America are also inconsistent [10,39,40,42,49]. One factor that may influence the $TPM_{2.5}$ cycle is the vertical gradient of $TPM_{2.5}$ concentrations [40]. If surface $TPM_{2.5}$ concentrations are fairly low, and if there is dry deposition in the nocturnal boundary layer, $TPM_{2.5}$ may increase in the morning when vertical mixing brings more $TPM_{2.5}$ from aloft. This is consistent with an increase in concentrations in the morning and stable concentrations during the day, as at Halifax (though as noted, the differences are small). In contrast, if there are local emissions, $TPM_{2.5}$ levels may build up during the night and drop in the morning. This pattern was not seen at any of the sites presented here. In an alternative mechanism, increased RGM (from photo-oxidation of GEM) may increase $TPM_{2.5}$ during the day if some of the RGM is scavenged by particles. This would be consistent with patterns at Dorset, Kejimkujik,

Genesee, and Alert. However, it should be noted that mean $TPM_{2.5}$ concentration at Alert are dominated by March and April peaks, while RGM concentrations are dominated by May values. Nevertheless, the photo-oxidation that produces high RGM in May likely produces high $TPM_{2.5}$ in March and April, when there is more particulate matter available and temperatures are colder [22], such that the diel cycles are similar. The diel cycle in $TPM_{2.5}$ at Churchill is opposite the diel cycle in RGM, suggesting that reactive Hg species generated during AMDEs around this site partition between the gas and particle phase depending on the temperature, with more adsorbed to particles during the cooler night hours. The erratic changes in all speciated Hg measurements from one hour to the next are a function of the short measurement period and the high variability in concentrations as AMDEs begin and end.

As expected—since GEM comprises the bulk of TGM—diel cycles in GEM are similar to those of TGM discussed above, with maximum amplitudes of 3%–9%. All but two sites (Mississauga and Alert) exhibited the typical non-urban diel cycle of minimum GEM at dawn and maximum GEM at mid-day or early afternoon. GEM in Mississauga followed the opposite cycle, with low values during the day and higher concentrations at night. This is more typical of urban sites, where local emissions build up TGM levels in the nocturnal boundary layer until they are diluted by cleaner air during the day when there is more mixing from aloft [12,40,42].

2.3. Seasonal Patterns in Atmospheric Hg and Hg in Precipitation

In Figure 7, monthly median TGM concentrations are plotted for the 11 sites with at least five years of data. Sites with shorter data coverage periods were excluded for clarity, but their cycles are discussed here. The data from the Lake Ontario Buoy reflect only three months of measurements and thus is not included in the overall seasonal discussion. At 12 of the 21 remaining sites (Reifel Island, Fort Chipewyan, Genesee, Esther, Burnt Island, St. Andrews, Kejimkujik, Egbert, Point Petre, Bratt's Lake and St. Anicet), maximum TGM concentrations are seen in late winter/early spring (February, March or April) and minima in the fall (September or October). This finding is consistent with previous results from Canada [8,9,11] and throughout the Northern Hemisphere [12,39,40,50]. This dominant pattern has previously been attributed to multiple factors, such as enhanced winter emissions from anthropogenic sources (primarily coal burning, as well as wood combustion), less vertical mixing in winter to clean out TGM that is emitted from surface sources [11,12], and increased oxidation and precipitation in summer [51,52]. However, modelling indicates that oxidation and precipitation are not significant factors in the TGM seasonality [23]. Rather, high revolatilization of Hg from snow significantly elevates GEM concentrations in winter in mid-latitudes. The evasion of Hg from snow and other surfaces increases with increasing solar radiation; this may cause the maximum in GEM to be in late winter /spring. In addition, several studies have shown that soil-air Hg emissions can be greatly enhanced as a result of warming temperatures [53] and increased soil moisture [54–57] that can occur following snowmelt. Terrestrial and oceanic emissions are at a maximum in summer. Therefore, the minimum in GEM concentrations generally occurs in fall when these various emission processes are least active. Five additional sites, not shown in Figure 7 (Saturna, Whistler, Little Fox Lake, Meadows and Mingan), had seasonal patterns similar to the dominant one discussed above, with slight differences in timing likely due to greater variability within these shorter measurement periods.

Alert showed the strongest seasonality with a minimum in the spring (April/May), maximum in the summer (July) and average concentrations in the fall and winter [13]. The spring depression is consistent with the AMDEs that occur at this site and the summer maximum is likely due to emission from various sources [13,29]. Kuujjuarapik also shows a summer maximum resulting from similar emissions as Alert, but the minimum is broader, extending from October to March. AMDEs in the spring at Kuujjuarapik are offset by rapid revolatilization of TGM after each event, resulting in no net depression of monthly TGM levels through the spring months.

Of the sites with less than five years of data, TGM concentrations at Southampton and Windsor, both with only two years of data, appear to have a bimodal seasonal pattern with low values of TGM in the spring and fall and high values in the summer and winter. The reason for this seasonality at Southampton is currently unclear for this relatively short and highly variable time series of data. Pollution episodes at Windsor are responsible for the summer maximum there. Similarly, Point Petrie was previously reported to have a summer maximum in TGM concentrations due to periodic elevated concentrations of TGM in the summer [8,11]; measurements of TGM that cover a longer time period have shown the spring maximum reported here. Finally, Flin Flon shows much higher TGM concentrations than any other site, with maxima in spring (April) and summer (July) and minima in the late fall/early winter [19].

Figure 7. Seasonal cycles in total gaseous mercury (TGM) at the 11 sites with more than five years of data. Cycles from Alert and Kuujjuarapik differ from the dominant pattern and are therefore highlighted.

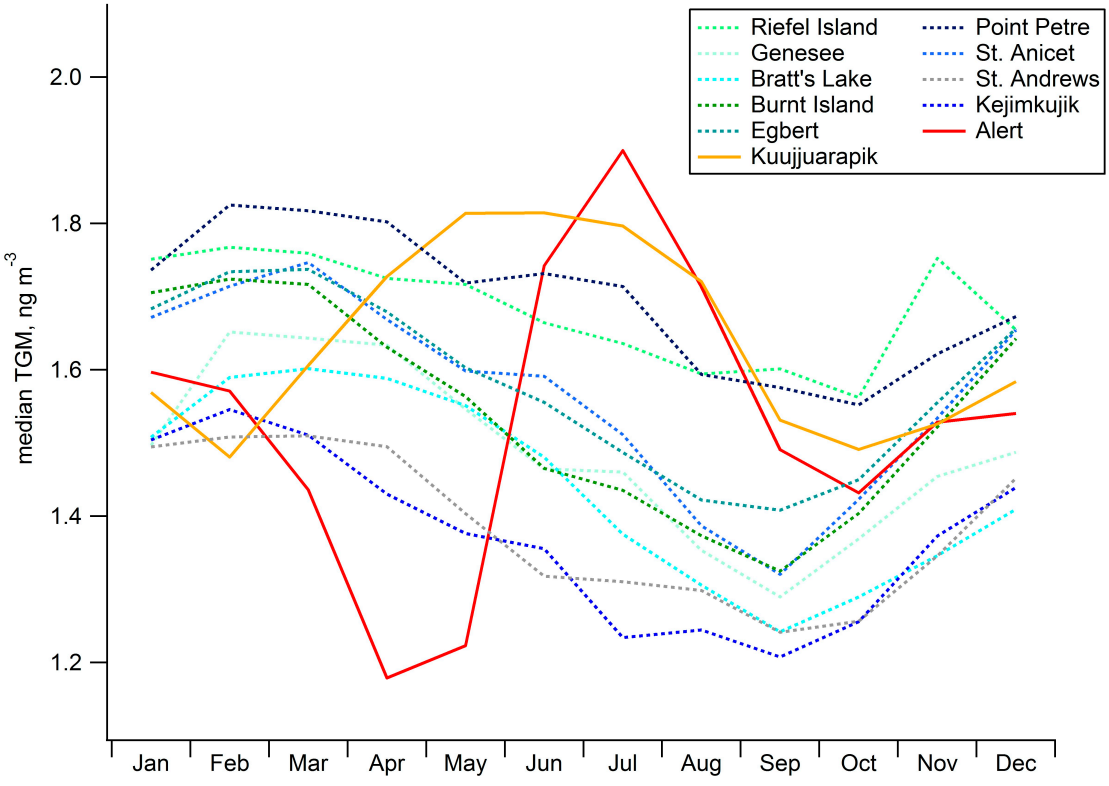

Seasonal variability in GEM, RGM and $TPM_{2.5}$ concentrations are shown in Figure 8. Of the 10 sites, three (Genesee, Flin Flon and Churchill) do not have measurements covering the entire year, so

discussion of seasonal cycles is limited by the data coverage at these sites. Flin Flon "seasonal" patterns may not be typical since speciated Hg measurements began in July, shortly after shut down of the copper smelter, which is likely why the highest GEM, RGM and $TPM_{2.5}$ concentrations were measured in July. Results from Flin Flon are discussed in detail elsewhere [19].

As shown in Figure 8, GEM concentrations at the remaining nine sites follow similar patterns to TGM concentrations as expected (since TGM is largely GEM). Four of the sites (Genesee, St. Anicet, Kejimkujik, Alert) also have TGM instruments and the cycles in GEM agree with the TGM cycles discussed above. Measurements at Churchill cover March through August and were lowest in March and April and highest in June due to AMDE chemistry, similar to Alert. The remaining four sites had maximum GEM concentrations in March (Mississauga, Dorset, Halifax) or April (ELA) and minimum GEM concentrations in August (Dorset), September (ELA) or October (Mississauga, Halifax). These cycles are in agreement with the dominant TGM patterns across the country as discussed above.

Figure 8. Seasonal cycles in speciated Hg (mean values for each month) at nine sites. Axis scales for RGM and $TPM_{2.5}$ vary.

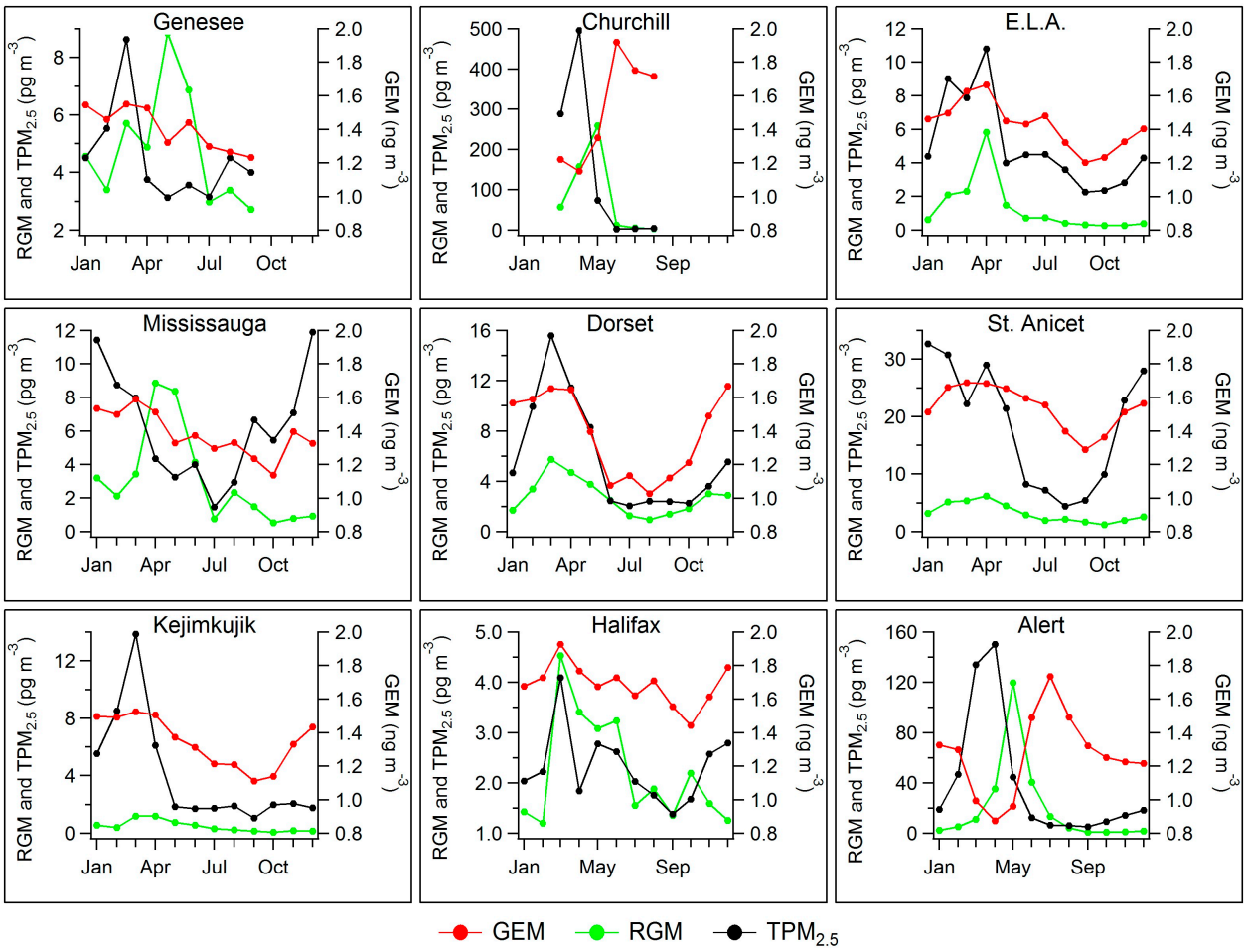

RGM concentrations were highest in the spring (March, April, or May) at all sites. Minimum RGM concentrations occurred in September or October at most sites, with the exceptions of Dorset (August) and Halifax (December–February). At Alert and Churchill, RGM was elevated in springtime due to AMDE activity. While the photo-oxidation of GEM to produce RGM is expected to be highest in

summer in other parts of the country due to more irradiation and oxidants, increased deposition of RGM may offset this increased source. Wet deposition of total Hg is highest in summer at most sites (see below) and dry deposition is expected to be much higher during summer and fall when vegetation is in full leaf [58]. Another factor may be a sampling artifact in the measurement of RGM, in which high concentrations of ozone in sampled air interfere with denuder absorption of RGM [34]. Since ozone concentrations are highest in summer, this artifact would suppress RGM concentrations the most during summer [59].

$TPM_{2.5}$ concentrations, like RGM, were high in March and April at the sites where AMDEs occur (Alert and Churchill) (Figure 8). Five non-AMDE sites also saw maximum $TPM_{2.5}$ concentrations in these months: Genesee, ELA, Dorset, Kejimkujik and Halifax. Mississauga and St. Anicet had elevated $TPM_{2.5}$ concentrations throughout the winter, peaking in December and January. These two sites are fairly close to urban centres, and may be affected by local and regional emissions that can be trapped close to the surface in the winter when mixing heights are low. $TPM_{2.5}$ may also be enhanced in cold months due to the gas-particle partitioning of semi-volatile Hg(II) species favouring the particle phase at low temperatures [60].

Finally, at many sites the peaks in GEM, RGM and $TPM_{2.5}$ coincide. This could point to common sources (such as coal combustion or other anthropogenic pollution at non-remote sites) or sinks (such as high summertime deposition) [11]. The interplay of various factors that may influence seasonal distributions of GEM, RGM and $TPM_{2.5}$ highlight the need for detailed modelling of these species in the atmosphere to explain these observations and determine their fate with respect to deposition.

The seasonal patterns of total Hg concentrations in rain and snow, precipitation amounts, and wet deposition of Hg at 22 sites were calculated by summing weekly samples over each calendar month. Monthly values were then averaged over all years of sampling. The seasonal pattern of Hg wet deposition showed maximum deposition in the summer (May–August) at 20 of 22 sites. The exceptions, Reifel Island and Dorset, had maxima in October and September, respectively. Twelve of the 22 sites reported here recorded less than three years of data, which increases the uncertainty in the seasonal cycling because there can be large inter-annual variability in precipitation amounts.

Seasonal cycles for four of the ten sites with at least three years of data are shown in Figure 9, illustrating representative patterns from those ten sites. Since Hg wet deposition flux depends on the total monthly precipitation amount and the concentration of total Hg in that precipitation, the seasonal cycles of both these parameters are shown along with the cycles of Hg wet deposition. For the sites not shown, seasonal patterns at Genesee and Henry Kroeger were similar to those at Bratt's Lake; patterns at St. Anicet, Mingan and Cormak resembled those at Egbert; patterns at St. Andrews were similar to those at Kejimkujik. The summer maximum in Hg wet deposition is predominant. However, examining patterns of total Hg concentrations and precipitation amount reveal that at Bratt's Lake, the Hg wet deposition maximum corresponds to the maximum in precipitation amount, whereas at Kejimkujik the maximum Hg wet deposition occurs during the season of minimum precipitation but highest total Hg concentrations. At Egbert, a peak in both total Hg concentrations and precipitation volume inevitably results in a period of maximum wet deposition. The pattern at Reifel Island indicates that the amount of precipitation is the dominant factor in determining the wet deposition cycle at that site.

Figure 9. Seasonal cycles in monthly wet deposition (black), precipitation amounts (gray bars), and concentration of total Hg in precipitation (red) at four sites.

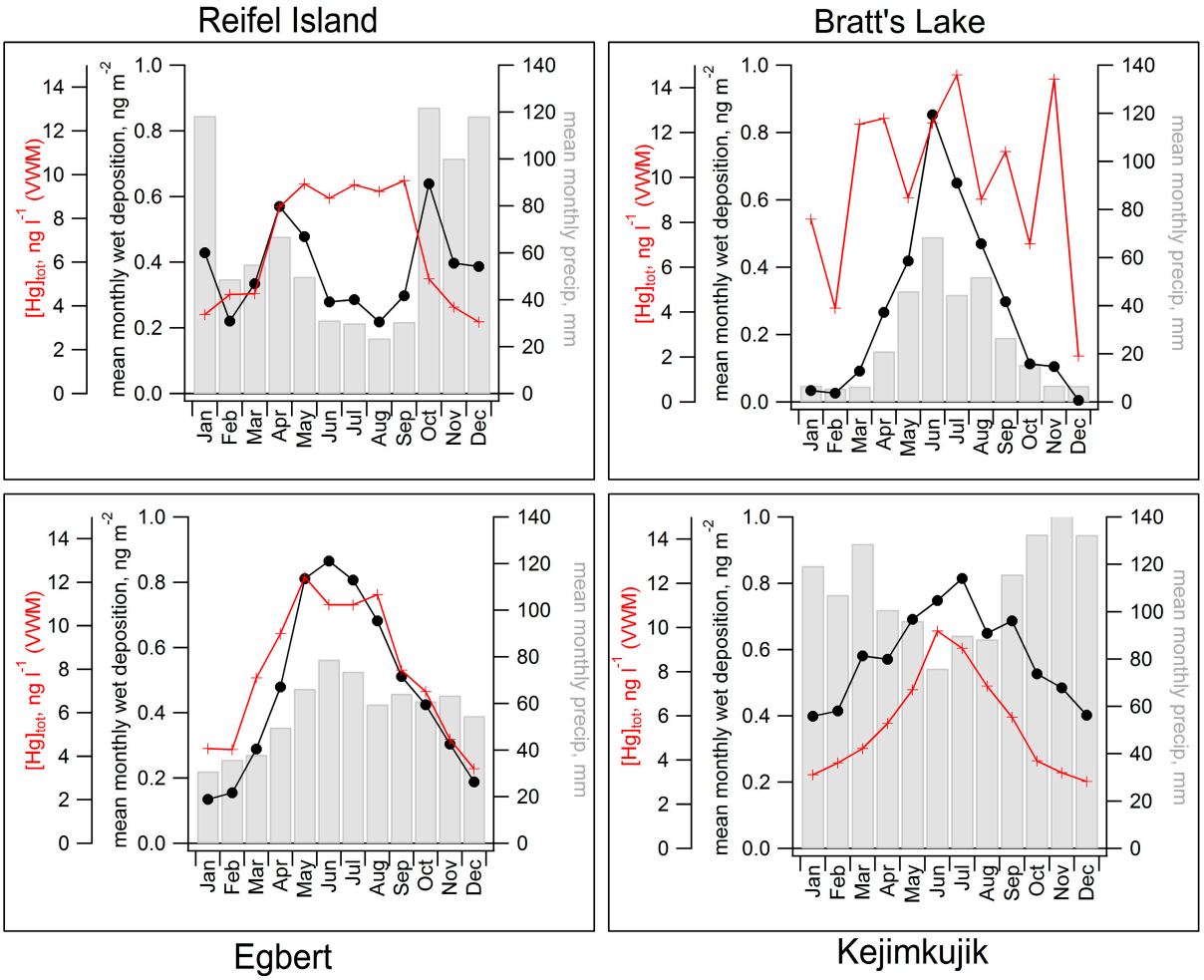

2.4. Long-Term Trends

Worldwide atmospheric measurements of TGM up to the early 2000s suggest that concentrations of atmospheric Hg increased from the 1970s to a peak in the 1980s and then plateaued in the late 1990s [24]. Similarly, measurements of air bubbles in a Greenland glacial firn indicated that GEM (the primary component of TGM) increased from the 1940s to the 1970s and reached a plateau around the mid-1990s [61]. In Canada, long-term trends in TGM [7,9,13,26], speciated atmospheric Hg [26] and Hg concentrations in precipitation [16,62] have been reported at some sites. The Canadian trends presented below are updated with the most comprehensive and recently available TGM, precipitation and Hg speciation data. The time period over which data is reported differs for each location. Linear trends were estimated for all available data from each site rather than limiting the analysis to only overlapping time periods. A minimum of five years of data were required to perform the Seasonal Kendall trend analysis, which is described in Section 3.

For TGM, the analysis used monthly median concentrations with the requirement that 75% of the month had valid data. Overall trend results for all sites with more than five years of data are listed in Table 4. Ten of the 11 sites experienced concentration decreases ranging from −0.9% to −3.3% per year, though time periods varied between five and 15 years. These decreases are comparable to a

reported trend in background TGM concentration at Mace Head, Ireland of −1.8% ± 0.1% per year over the period 1996–2009 [63]. The six sites that best overlap with that time period (Egbert, Point Petre, St. Anicet, St. Andrews, Kejimkujik and Alert) recorded decreases of 0.8%–1.8% yr^{-1}. In contrast, TGM in the southern hemisphere declined at a faster rate of approximately −2.7% per year from 1996 to 2009, based on data from shipboard measurements and monitoring at Cape Point, South Africa [25]. Of the eleven sites, only Genesee, where measurements began in 2004, did not have a significant decrease in TGM over the measurement period.

Table 4. TGM trends (and 95% confidence limits) at sites with >5 years of measurements.

Site	Time Period	TGM Trend, $pg \cdot m^{-3} \cdot yr^{-1}$	TGM Trend, % yr^{-1}
Reifel Island	1999–2004	−55 (−70 to −40)	−3.3 (−4.2 to −2.4)
Genesee	2004–2010	−6 (−21 to +1) (ns)	−0.4 (−1.4 to +0.1) (ns)
Bratt's Lake	2001–2010	−37 (−48 to −23)	−2.5 (−3.4 to −1.6)
Burnt Island	1998–2007	−15 (−22 to −7)	−1.0 (−1.4 to −0.4)
Egbert	1996–2010	−20 (−27 to −16)	−1.3 (−1.7 to −1.0)
Kuujjuarapik	1999–2009	−40 (−55 to −23)	−2.4 (−3.4 to −1.4)
Point Petre	1996–2007	−29 (−38 to −20)	−1.7 (−2.2 to −1.2)
St. Anicet	1995–2009	−24 (−29 to −19)	−1.5 (−1.8 to −1.2)
St. Andrews	1996–2007	−30 (−42 to −20)	−2.2 (−3.1 to −1.5)
Kejimkujik	1996–2010	−14 (−20 to −6)	−1.0 (−1.4 to −0.5)
Alert	1995–2011	−14 (−18 to −10)	−0.9 (−1.1 to −0.6)

Seasonal trend analysis for TGM is exemplified for two sites—Reifel Island and Kejimikujik—in Figure 10. An overall decreasing trend of $-0.055\ ng \cdot m^{-3} \cdot yr^{-1}$ or $-55\ pg \cdot m^{-3} \cdot yr^{-1}$ was determined at Reifel Island from five years of data. To illustrate the result, the time series of monthly median TGM is shown in the bottom of Figure 10 where the red line indicates the slope. The results from Kejimkujik show that even in a data set that has greater seasonal variability, a longer time period narrows the uncertainty in the seasonal trends and the differences between months.

An earlier analysis by Temme *et al.* [9] using a different statistical technique found significant declines in TGM at Burnt Island, Egbert, Point Petre, St. Anicet, St. Andrews and Kejimikujik and no significant change at Reifel Island, Bratt's Lake and Alert, based on measurements to 2005. The trends reported here with an additional 3–5 years of monitoring agree (within uncertainties) with the earlier trends at three sites (Burnt Island, Point Petre, St. Anicet) and show an increasingly negative trend at Reifel Island, Bratt's Lake, Egbert, St. Andrews, Kejimkujik and Alert.

Anthropogenic emissions of Hg from Canada and the United States, which decreased by approximately 60%–70% from 1995 to 2010, contribute roughly 15% or less of the TGM measured at Canadian sites, depending on the relative amounts of anthropogenic, natural and legacy (re-emissions of previously-deposited mercury) emissions [62,64,65]. Regional emission decreases may therefore account for approximately 0.5%–1% yr^{-1} in TGM concentration changes, at least in the eastern mid-latitudes where most of the sources are located. Since the bulk of TGM in Canada is from global and natural sources, the magnitude of the concentration decline is inconsistent with global emission estimates for the past 15 years that suggest that global anthropogenic Hg emissions have increased [66]. If these emission budgets are accurate, then either surface (natural and legacy)

emissions have decreased or there has been increased deposition of Hg, either globally or near emission sources. The following sections discuss long-term trends in RGM and $TPM_{2.5}$ (which contribute to both wet and dry deposition fluxes) and trends in measured wet deposition of Hg.

Figure 10. Long-term trends in TGM by season (**top**) and monthly median TGM with overall annual trend (**bottom**), at Reifel Island and Kejimkujik

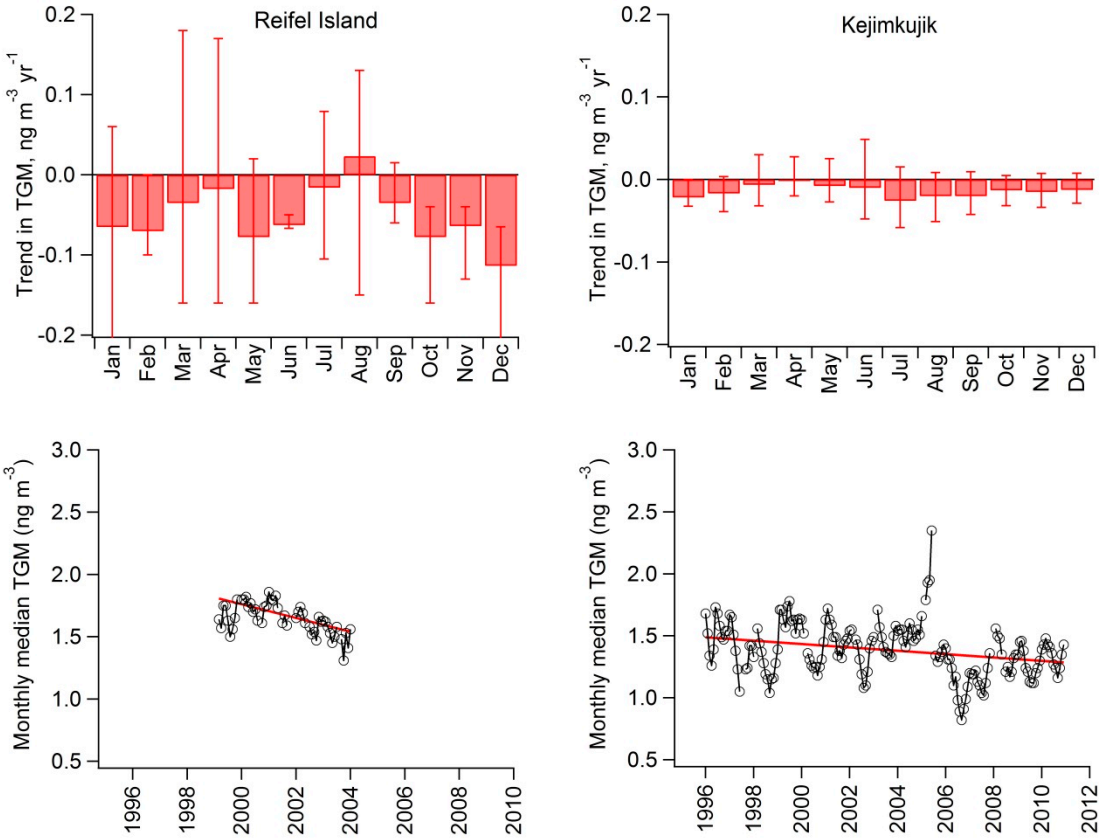

Three sites in Canada—Alert, St. Anicet and ELA—have been collecting speciated Hg data for more than five years as shown in Figure 11. Daily mean concentrations of RGM, $TPM_{2.5}$ and GEM were used to calculate seasonal trends at these sites in months with sufficient valid data. The results of these calculations are shown in Figure 12, where a positive trend indicates a year-to-year increase in concentration for that month. While an overall trend was not reported for this data due to insufficient data in some months, a few interesting features in the seasonal trends were observed for RGM, $TPM_{2.5}$ and GEM, as discussed below.

For the Alert data, which showed significant amounts of RGM from February to July, the highest concentrations every year were seen in the month of May, with a median concentration of 110 $pg \cdot m^{-3}$. Measurements from May over the ten years of monitoring have shown an RGM increase of 7.5 ± 3.5 $pg \cdot m^{-3} \cdot yr^{-1}$, or 6.8% per year. Concentrations of RGM in April and July also increased significantly, though the absolute changes were much smaller than in May due to lower levels of RGM. No significant trends were seen in the March and June RGM data. RGM measurements at St. Anicet and the ELA were below estimated detection limits for most of the year and thus trends are not reported for those sites. In general, seasonal trends were not calculated for months in which more than half of the measurements were below instrumental detection limits or for months that did not have

measurements covering at least 75% of the days in that month for at least five years. It should be noted that further investigation into the detection limits of these instruments (discussed in Section 3) may validate more of the existing data and allow additional trends to be calculated in the future.

Figure 11. Reactive gaseous mercury (RGM) and total particulate mercury ($TPM_{2.5}$) at sites with more than five years of monitoring.

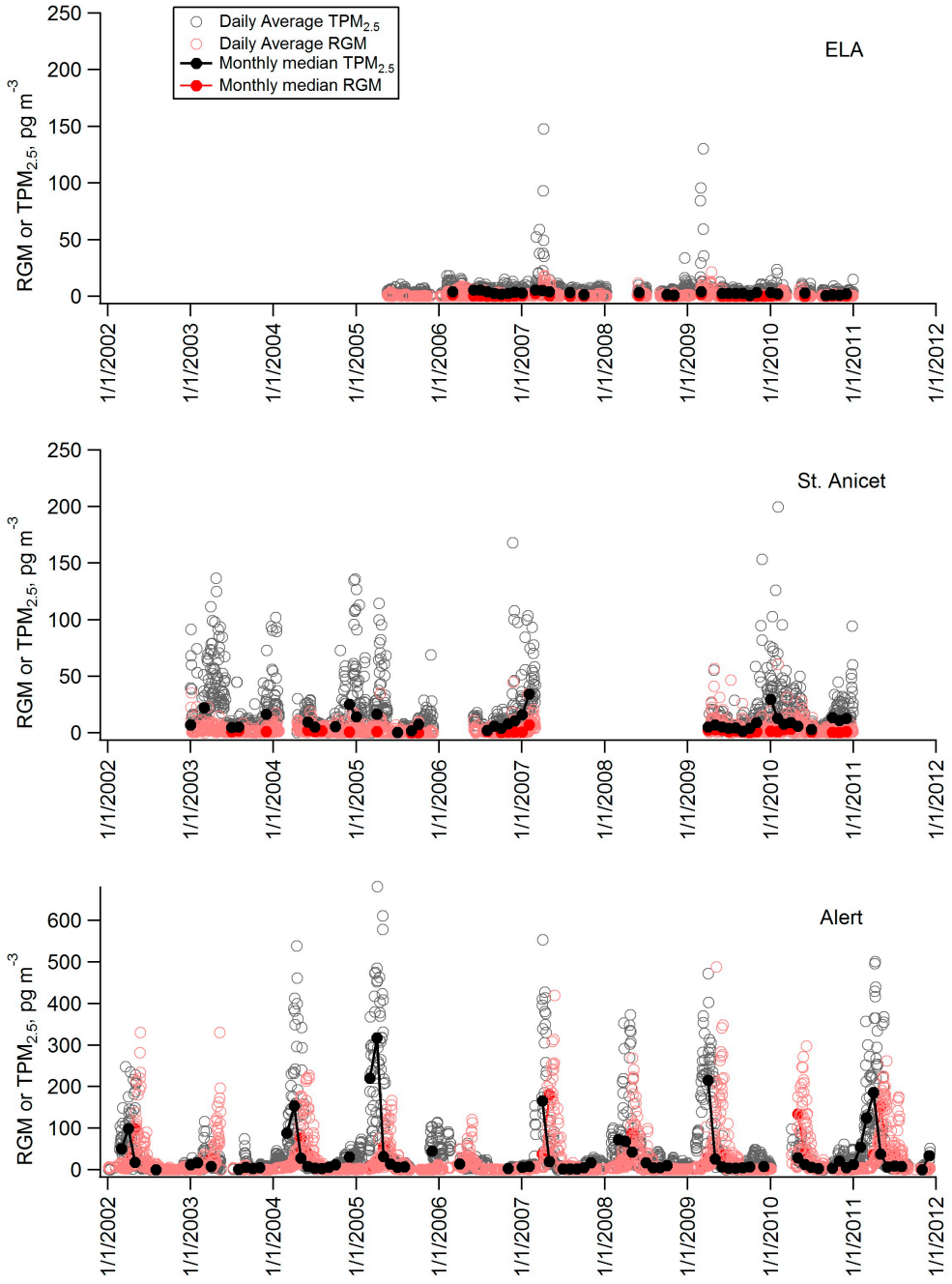

In contrast, measurements of $TPM_{2.5}$ are generally higher than RGM at these locations and therefore a few more valid monthly trends were reported in the seasonal trend analysis. Trends were variable and, for the lower latitude sites, found to be significant in both positive (increasing) and negative (decreasing) directions depending on the month. At the ELA, $TPM_{2.5}$ decreased in June, the only month with sufficient data coverage. At St. Anicet, $TPM_{2.5}$ decreased in July, increased in October and

January, and did not show a significant trend in December. The magnitude of these trends ranged from −0.2 to +1.6 pg·m^{-3}·yr^{-1} or −3 to +12% yr^{-1}. At Alert, $TPM_{2.5}$ showed a significant increase in the months where concentrations were the highest overall, namely March and April. The increase in March was 10 ± 6 pg·m^{-3}·yr^{-1} (10% yr^{-1}) and in April was roughly 7 pg·m^{-3}·yr^{-1} or 7% yr^{-1}, based on median concentrations of 99 and 98 pg·m^{-3}, respectively. Trends in the remainder of the months were either positive (May, July, August) or not significant. As with RGM, no negative trends in $TGM_{2.5}$ were observed at Alert.

Figure 12. Seasonal trends in RGM, $TPM_{2.5}$ and GEM at the three sites with >5 years of speciation measurements. A positive trend indicates a year-over-year increase in concentrations for that month. Note scale change for GEM.

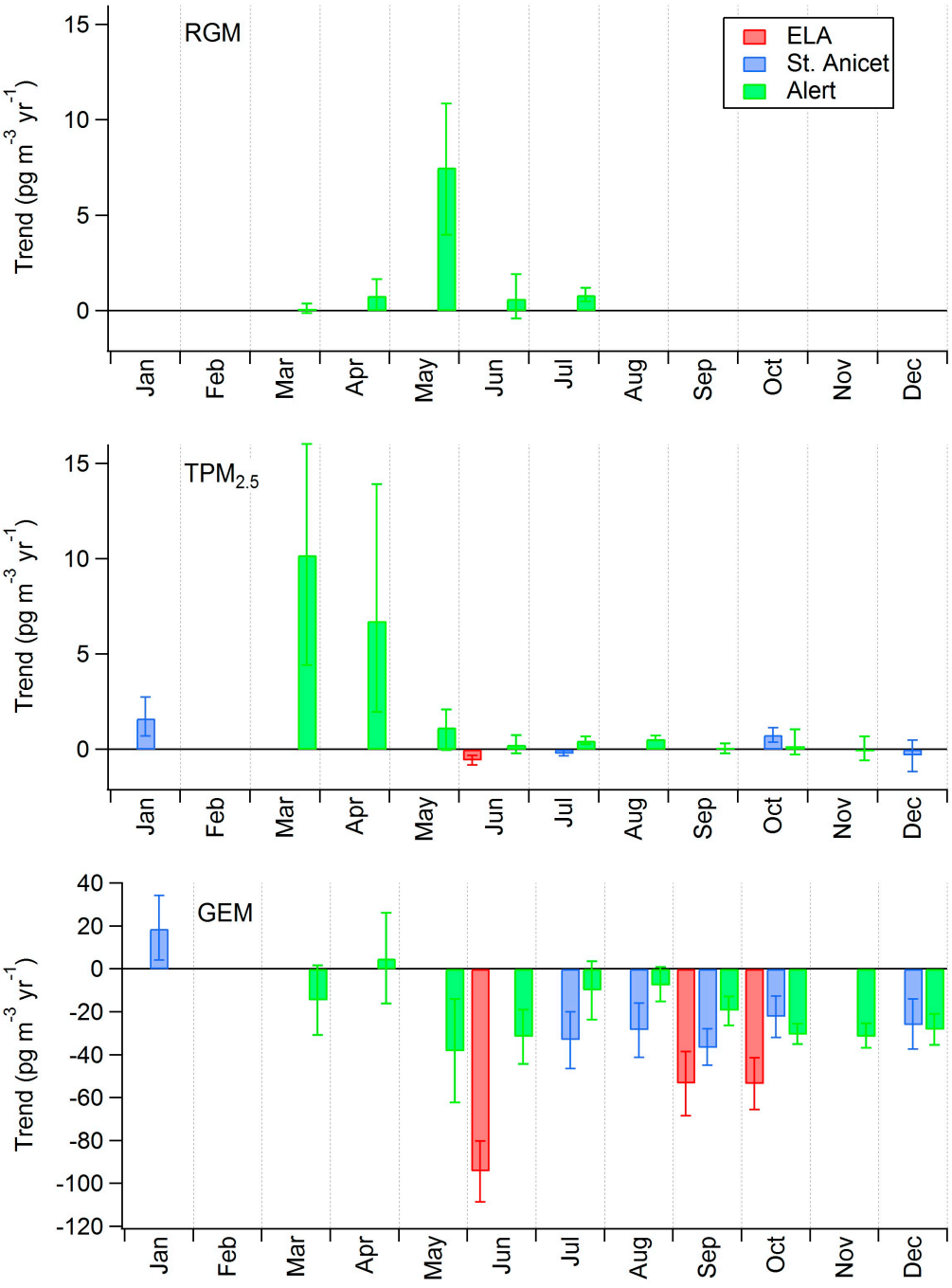

The overall decreasing trend of TGM reported from across the country is also evident in the GEM measurements at the ELA and in most months for St. Anicet and Alert. The latter two sites show more variability in the GEM than TGM trends at the same sites. This is likely due to a shorter measurement period for this speciation data compared to the TGM data.

The springtime trends in speciated Hg at Alert are of interest because of their link to atmospheric photochemistry and ocean conditions at this time of year. An increase in RGM and $TPM_{2.5}$ during the AMDE season could indicate an overall increase in the amount of oxidation of GEM by halogen radicals. However, trends in GEM over the same period are not consistently decreasing (GEM decreased in May but did not change significantly in March or April) as would be expected from an increase in the oxidation rate. Also, these trends are still qualitatively uncertain due to the short time period and the fact that RGM and $TPM_{2.5}$ measurements are still not well-calibrated.

A long-term trend study from Resolute Bay, NU, was based on observations of filterable Hg (manual samples of Hg collected by passing air through particle filters which likely reflects the sum of $TPM_{2.5}$ and RGM combined) from 1974 to 2000 [67]. These authors reported a decrease of approximately 3% per year in total filterable Hg in summer and fall which is similar to the world-wide decrease in Hg emissions from anthropogenic activities between 1983 and 1995 and with reports on other atmospheric data [24]. Considerable variability was found in the data during the winter and early spring months suggesting some influence of AMDEs in the samples. These data precede the continuous measurements presented here and suggest that trends may be changing in recent decades.

To assess changes in the wet deposition of Hg, trends were calculated for the volume-weighted monthly mean concentration of total Hg in precipitation, the total monthly precipitation volume and the resulting monthly wet deposition Hg flux. Data from Egbert, St Anicet, St Andrews, Kejimkujik, Mingan and Cormak are reported because gaps in data from Bratt's Lake and Henry Kroeger limited the trend calculation using this technique.

The results are shown in Figure 13 and reveal that trends in Hg wet deposition at all sites are not significantly different from zero (95% confidence limits). Four sites report a significant decrease in the concentration of total Hg in precipitation (Egbert, St. Anicet, St. Andrews, and Kejimkujik). Mingan and Cormak had decreases that were not significantly different from zero. Overall deposition is a function of both Hg concentration and amount of precipitation, as seen at St. Anicet where a decrease in Hg concentration and an increase in precipitation amount resulted in a non-significant change in the wet deposition of Hg. Using a different statistical method, a similar result (no change in wet deposition flux of total Hg) was seen at ELA from 2001 to 2006 [35].

Overall time trends for Hg concentrations in precipitation are compared with those reported through the Mercury Deposition Network (MDN) in Table 5. The MDN results reported in 2009 are based on data up to 2005 [16]. The St. Andrews trend reported for the period 1996–2003 is small but decreasing and shows the strongest time overlap between trend analyses. However, some inconsistencies were found for the 2002 concentration between the 2009 publication and the MDN website and thus the trend value is flagged. At Egbert, the trend from the current analysis found a significant decrease of $-2.1\%\ yr^{-1}$, which differs from the "no trend" reported earlier and is consistent with a recent report of a significant decrease between 2004 and 2010 [62]. At Cormak, the new ten-year trend is decreasing at a slower rate, $-1.7\%\ yr^{-1}$, than the previous five-year trend, $-4.4\%\ yr^{-1}$, and is not significant at the 95% confidence level. Finally, trends reported from St. Anicet, Kejimkujik and Mingan have not

changed significantly with the addition of more recent data. For these six sites, additional tests for spatial homogeneity, similar to the seasonal homogeneity tests, were performed to test if there was an overall trend across eastern Canada. Results showed that trends for wet deposition, Hg concentrations and precipitation amounts were homogeneous between the sites. As expected from individual site results, trends in wet deposition flux and precipitation amounts for the entire group were not significantly different from zero. Only Hg concentration in precipitation had a significant trend for the group, with an overall decrease estimated at -0.13 ± 0.04 ng·L^{-1}·yr^{-1} or $-2.1 \pm 0.6\%$ yr^{-1}.

Figure 13. Overall trends in wet deposition, Hg concentration, and total precipitation at six sites with >5 years of Hg precipitation measurements.

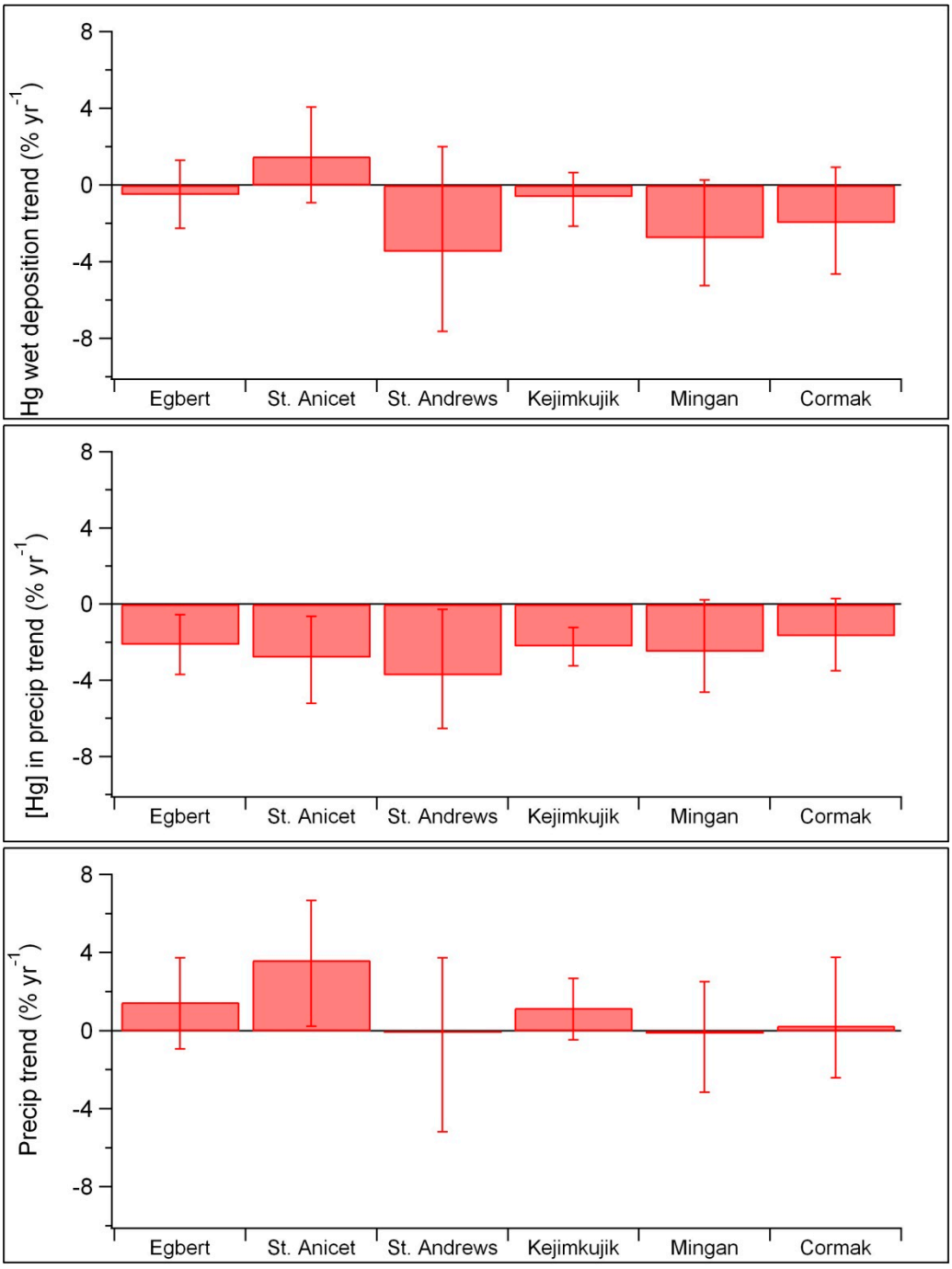

At the two long-term sites in western Canada, Bratt's Lake and Henry Kroeger, low precipitation levels in the winter resulting in few data points restricted both the performance of a seasonal Kendall test and determination of an overall trend. However, a standard Mann-Kendall test for trend was performed over the entire time period and revealed no significant trend in Hg wet deposition or Hg precipitation concentrations at either site.

Table 5. Trends (with 95% confidence limits) in total Hg in precipitation at sites with >5 years of measurements, as well as results from Prestbo and Gay (PG) 2009. Concentrations are volume weighted means (ns = not significant).

Site	Time Period	[Hg] Trend, $ng \cdot L^{-1} \cdot yr^{-1}$	[Hg] Trend, % yr^{-1}	Time Period (PG 2009)	[Hg] Trend (PG 2009), % yr^{-1}
Egbert	2000–2010	−0.18 (−0.31 to −0.05)	−2.1 (−3.7 to −0.6)	2000–2005	ns
St. Anicet	1998–2007	−0.22 (−0.41 to −0.05)	−2.8 (−5.2 to −0.6)	1998–2005	−1.5
St. Andrews	1996–2003	−0.25 (−0.43 to −0.02)	−3.7 (−6.5 to −0.3)	1997–2003	−1.9 **
Kejimkujik	1996–2010	−0.12 (−0.17 to −0.06)	−2.2 (−3.3 to −1.2)	1997–2005	−2.0
Mingan	1998–2007	−0.13 (−0.23 to +0.01) ns	−2.5 (−4.6 to +0.2) ns	1998–2005	ns
Cormak	2000–2010	−0.07 (−0.15 to +0.01) ns	−1.7 (−3.5 to +0.3) ns	2000–2005	−4.4

** Possible error in data set.

Four of the long-term precipitation collection sites also measure TGM (Egbert, St. Anicet, St. Andrews and Kejimkujik). A comparison of the TGM concentrations in air and Hg concentrations in precipitation shows that they have both significantly decreased at all four sites. Quantitatively comparing the trends, trends in TGM concentration at Egbert, St. Anicet and St. Andrews agreed with trends in precipitation concentrations within the uncertainties, though measurement time periods were not identical. At Kejimkujik, the rate of decrease of Hg concentration in precipitation (−2.2% yr^{-1}) was significantly more negative than the decrease in TGM concentration (−1.0% yr^{-1}) over the same time period. Similar results were reported for earlier trend comparisons [9]. These differences suggest there may be changes in precipitation amounts or types, and/or in the distribution of GEM, RGM and $TPM_{2.5}$ (which are scavenged with differing efficiencies).

The wet deposition trends presented here for Canada as well as those for the United States [16,62] do not show a large-scale increase in wet deposition of Hg in eastern mid-latitude North America. Therefore, the additional decreases observed in TGM concentrations at these Canadian sites (on top of those due to regional emission controls) cannot be explained by increased wet deposition in this region as might be expected if changes in Hg speciation or precipitation were scavenging more Hg from the atmosphere. Increased deposition in other areas could have offset increasing global anthropogenic emissions; increased monitoring of wet deposition in under-sampled areas, such as ecologically sensitive northern regions, is needed to provide model constraints and track the response of the Arctic and sub-Arctic to changes in emissions and climate. Alternatively, significant decreases in natural emissions [25,68] or in re-emissions of recently deposited Hg could also result in a declining trend in air concentrations.

3. Methods

3.1. Data Collection

TGM measurements were made using automated Tekran® 2537 Hg vapour analyser [9,27,69]. The air is sampled at flow rates between 1.0 and 1.5 L·min^{-1} through a Teflon filter (47 mm diameter; 0.2 μm pore). The Hg in the sample air is pre-concentrated by amalgamation on two gold cartridges (5–30 min pre-concentration times) which alternate between collection and thermal desorption and detection for continuous monitoring. Elemental Hg is detected using Cold Vapour Atomic Fluorescence Spectrometry (CVAFS). The instruments are calibrated daily using an internal Hg permeation source and verified during routine site audits by manual injections of Hg from an external source. The data are quality controlled using the Environment Canada Research Data Management and Quality Control (RDMQ) system [70]. Limited studies suggest that TGM measurements consist of GEM and RGM [71,72]; however it is possible that under certain environmental conditions and sample inlet configurations, the RGM is removed.

Speciated Hg measurements (GEM, RGM and $TPM_{2.5}$) were made using Tekran® Mercury 1130, 1135 and 2537 speciation systems and are described in detail elsewhere [27,73]. Briefly, air is pulled into the analyzer through a Teflon® coated elutriator and impactor designed to remove particles >2.5 μm at flow rates of 10.0 L·min^{-1}. The sample air flows over a KCl coated quartz denuder to trap the RGM in the 1130 unit and then passes over a quartz particulate filter to trap $TPM_{2.5}$ in the 1135 unit. The remaining GEM is carried into the 2537 analyser (at a flow rate of 1 L·min^{-1}) for analysis. RGM and $TPM_{2.5}$ are accumulated at a high flow rate for 1 to 3 h while the GEM is collected every 5 minutes. RGM and $TPM_{2.5}$ are subsequently thermally desorbed and pyrolysed to GEM and then analysed by the 2537, interrupting the sampling. Exact identification of RGM and $TPM_{2.5}$ fractions are still not known and thus are operationally defined. Therefore, in lieu of RGM and $TPM_{2.5}$ standards, rigorous procedures during and after sample collection/analysis have been put in place to ensure standard methods are used at all site locations [70].

The analytical detection limit of GEM in the Tekran 2537 is <0.1 ng/m^3 in 7.5 L, or <0.75 pg. Therefore, detection limits for RGM and $TPM_{2.5}$ in the 2537 alone would be <0.4–1.2 pg·m^{-3} (depending on the collection time), though the manufacturer estimated 2 pg·m^{-3} as the more reasonable limit. Detection limits ranging from 1 to 3 pg·m^{-3} for RGM and $TPM_{2.5}$ were determined at particular sites with multiple years of measurements using three times the standard deviation of the blanks (zero-air samples) during each desorption cycle. Discussions regarding determination of the instrument detection limits are currently ongoing within the research community. For individual RGM and $TPM_{2.5}$ measurements the RDMQ process validates/invalidates measurements taking into consideration the magnitude of the species concentrations relative to the blank values for each desorption.

Precipitation samples were collected according to the Mercury Deposition Network (MDN) SOP using an automatic precipitation sampler (Modified Aerochem Metrics Model 301 or N-Con Systems Co. Automatic Precipitation Sampler). The sampler was open to the atmosphere only during precipitation events that were detected using a sensor. The sampling system/train consists of a borosilicate glass funnel connected to an acid-cleaned, 3-mm capillary tube. The other end of the

capillary tube is expanded to form a sphere with a small hole that allows water to drain into a 2-liter borosilicate glass bottle that is pre-charged with dilute hydrochloric acid to prevent microbial activity and volatilization [16]. The sample collection system housing is insulated and temperature controlled. Field operators collect samples once a week using clean techniques and replace the entire sampling train with fresh equipment that that has been rigorously cleaned. All sample analysis and glassware cleaning is performed by the Mercury (Hg) Analytical Laboratory (HAL) at Frontier Global Sciences. The weekly precipitation amount is recorded for deposition determination using a precision precipitation gauge (Belfort Universal Precipitation Gauge 5–780 or NOAH IV, ETI Instrument Systems, Inc).

Precipitation samples were analysed at the laboratory using the EPA method 1631 to measure total Hg. Bromine chloride (BrCl) in hydrochloric acid (HCl) is added to the sample bottle to oxidize all forms of Hg to Hg^{2+}. Stannous chloride ($SnCl_2$) is added to reduce Hg^{2+} to Hg° and the sample is purged with ultra-pure nitrogen onto gold-coated silica traps. A dual gold trap amalgamation technique is used to concentrate and focus the Hg. The Hg is removed from the gold traps via thermal desorption and is analysed using CVAFS and quantified by peak height. Field blanks, system blanks and laboratory blanks are all routinely analysed as part of quality assurance procedures. The laboratory performs weekly standard reference material and spike recovery tests. Sample Hg concentrations are blank corrected and the method of detection limit is approximately 0.1 $ng \cdot L^{-1}$ based on three standard deviations of the laboratory blanks. All data is reviewed and validated by the Mercury Analytical Laboratory.

3.2. Data Analysis

Final data obtained from the National Atmospheric Chemistry database [74] or provided by principal investigators were first averaged to give daily values for TGM and speciated Hg concentrations and monthly values for wet deposition and volume-weighted mean concentrations in precipitation, with 75% data coverage required within the day or month for acceptance of the daily TGM or monthly precipitation average. Due to differing sampling intervals for speciation data, a minimum of three samples in a day was required to accept daily averages for GEM, RGM and $TPM_{2.5}$. Weekly precipitation samples that covered a change in the calendar month were partially attributed to each of the two months, weighting the sample in each monthly average (or sum) according to the number of days from that week that belonged to the month in question. Atmospheric speciation measurements that sampled over midnight were similarly treated. Daily/monthly averages were then used to calculate summary statistics for each site (see supplementary data file). Diel patterns were calculated for TGM using hourly averages, again requiring 75% coverage within the hour. Since speciated Hg concentrations used 1–3 h collection intervals, the start and end times of the collection period were rounded to the nearest hour and each hour within the adjusted start and end times was assigned the concentration value for that sample. No concentration was assigned during the analysis period.

Long-term trends were calculated using the seasonal Kendall test for trend and the related Sen's slope calculation [75]. This method is an extension of the non-parametric Mann-Kendall test for trend in which data from the 12 months are treated as 12 separate data sets. The Mann-Kendall test is

recommended for data sets in which there are missing points, which applies to many of the data sets used here, and when the data are not normally distributed, which is true for some sites (e.g., Alert). Non-parametric tests are also more robust for long-term trend analysis (compared to a parametric linear regression) since they are less sensitive to outliers at the beginning and end of the data set. For each month, the presence of a trend is confirmed or rejected by the Mann-Kendall test and a slope is estimated using Sen's nonparametric estimator of slope. An overall annual trend can then be estimated from the monthly trend statistics; however, this estimate is less reliable if the monthly trends are not sufficiently homogeneous. Thus, to ensure reliability of the data, a test for seasonal homogeneity was performed as well [76]. If seasonal trends were homogeneous, the results were used to determine an overall trend for the entire period. If they were not homogeneous, or when there were insufficient data to calculate a trend in certain months, only trends for individual months were reported.

4. Conclusions

A synthesis of all available Hg measurements from Canadian air and precipitation monitoring sites is presented, including diel and seasonal cycles and long-term trends. These results provide a wealth of data on long-term patterns in Hg species for validation of models of the transformation and deposition of atmospheric Hg. They also provide a baseline for evaluating the response of Hg concentrations and deposition to emission reduction strategies both nationally and under the Minamata Convention, an international agreement on Hg signed by 99 countries to date [77]. With broad geographic coverage including remote sites with few local or regional sources, Canada's observation network is well positioned to evaluate future Hg trends in the Northern Hemisphere.

TGM concentrations, with the exception of Flin Flon, were in the range of 1.2–1.9 $ng \cdot m^{-3}$ across the country, similar to northern hemispheric background levels. RGM and $TPM_{2.5}$ ranged from a few $pg \cdot m^{-3}$ over much of the country to hundreds of $pg \cdot m^{-3}$ during spring AMDEs at Alert and Churchill. Wet deposition amounts averaged between 0.1 and 0.8 $\mu g \cdot m^{-2} \cdot month^{-1}$, except at Flin Flon. Spatial patterns of Hg measurements showed the influence of local and regional sources and sinks. For example, high air concentrations of Hg species and higher Hg deposition were seen in the vicinity of the Flin Flon smelter and in the populated Great Lakes region, while AMDE chemistry in the spring and oceanic emissions in the summer influenced seasonal patterns in GEM, RGM and $TPM_{2.5}$ in Arctic and sub-Arctic locations.

At all sites in this survey, RGM levels were highest in the mid-afternoon. This pattern is consistent with photochemical formation of RGM and a relatively short lifetime (on the order of hours), though elevated levels of RGM persisted through the night in Churchill and Alert during the AMDE season, suggesting the lifetime may be longer depending on conditions. Other atmospheric Hg species had more diverse diel patterns. At remote sites, TGM and GEM were generally lowest in the early morning, as deposition in the shallow nocturnal boundary layer depleted TGM relative to the free troposphere above. Sites influenced by urban emissions and/or on- and off-shore breezes did not follow this pattern.

Seasonal patterns in TGM and GEM concentrations were similar at most mid-latitude sites, with maxima in the late winter or early spring and minima in the fall, perhaps due to surface evasion. Sites

influenced by AMDEs were the exception, with highest concentrations in the summer and lower in the spring (Alert) or winter (Kuujjuarapik). RGM levels peaked in the spring, in contrast to the summer maximum that might be expected due to its photochemical source. Increased wet and dry deposition, or analytical issues, may play a role. $TPM_{2.5}$ levels were also highest in spring at remote sites and in winter at more polluted locations. Wet deposition of total Hg was almost always highest in summer, except at Reifel Island, BC, where the dry summer months resulted in much lower wet deposition.

Concentrations of both TGM and Hg in precipitation have declined at most sites since the mid-1990s, while Hg wet deposition trends were not significant due to variability in precipitation amounts. The TGM trends extend the number of global sites reporting decreases over the last two decades [7,25,26,63]. Increases in springtime RGM and $TPM_{2.5}$ previously noted at Alert for 2002–2009 [26] are further supported by the additional two years of data included here.

Moving forward, in addition to continued monitoring, identification of the compounds making up RGM and $TPM_{2.5}$ and the development of calibration standards continue to be needed. Knowledge of these exact chemical species would also lead to improved understanding of the chemistry and wet and dry deposition rates of RGM and $TPM_{2.5}$ in different air masses. Wet deposition measurements in Arctic and sub-Arctic locations would assist modellers in constraining the atmospheric Hg budget in this vast area, as would additional direct measurements of dry deposition across the country.

Acknowledgments

Funding for CAMNet and CAPMoN was provided by Environment Canada (EC). Additional funding was provided by the Northern Contaminants Program (Aboriginal Affairs and Northern Development Canada), the Geological Survey of Canada, the Natural Sciences and Engineering Research Council, the Government of Canada Program for International Polar Year, EC's Global Atmospheric Watch program and Whistler program, and Manitoba Hydro. Additional data was contributed by the Meteorological Service of Canada Air Quality Unit in Edmonton and by Geoffrey Stupple. Thanks to the numerous former and current scientists and technicians for CAMNet and CAPMoN, particularly Steve Beauchamp, Cathy Banic, Keith Puckett for the creation of CAMNet; to Patrick Lee for support at other EC sites; to Greg Skelton and Tina Scherz for many years of data QC; to Mike Shaw for the site map; and to Heather Morrison and Pierrette Blanchard for coordinating this project for the Canadian Mercury Science Assessment.

Author Contributions

Amanda S. Cole created several figures and wrote the majority of the text, along with Alexandra Steffen. Julie Narayan generated statistics for a large part of the data as well as additional figures. Chris S. Eckley assembled and quality controlled several data sets and wrote parts of the experimental section. Rob Tordon collected data from St. Andrews, Kejimkujik, Cormak and Halifax and contributed to writing the experimental section. Data were collected and editorial input provided by Martin Pilote (St. Anicet, Mingan and Kuujjuarapik), Jennifer A. Graydon and Vincent L. St. Louis (ELA), Xiaohong Xu (Windsor) and Brian A. Branfireun (Mississauga and Dorset).

Conflicts of Interest

The authors declare no conflict of interest.

References

1. Selin, N.E. Global biogeochemical cycling of mercury: A review. *Ann. Rev. Environ. Resour.* **2009**, *34*, 43–63.
2. Corbitt, E.S.; Jacob, D.J.; Holmes, C.D.; Streets, D.G.; Sunderland, E.M. Global source-receptor relationships for mercury deposition under present-day and 2050 emissions scenarios. *Environ. Sci. Technol.* **2011**, *45*, 10477–10484.
3. Holmes, C.D.; Jacob, D.J.; Corbitt, E.S.; Mao, J.; Yang, X.; Talbot, R.; Slemr, F. Global atmospheric model for mercury including oxidation by bromine atoms. *Atmos. Chem. Phys.* **2010**, *10*, 12037–12057.
4. Lindberg, S.; Bullock, R.; Ebinghaus, R.; Engstrom, D.R.; Feng, X.; Fitzgerald, W.F.; Pirrone, N.; Prestbo, E.; Seigneur, C. A synthesis of progress and uncertainties in attributing the sources of mercury in deposition. *Ambio* **2007**, *36*, 19–32.
5. Schroeder, W.H.; Munthe, J. Atmospheric mercury—An overview. *Atmos. Environ.* **1998**, *32*, 809–822.
6. Hynes, A.J.; Donohoue, D.L.; Goodsite, M.E.; Hedgecock, I.M. Our current understanding of major chemical and physical processes affecting mercury dynamics in the atmosphere and at the air-water/terrestrial interfaces. In *Mercury Fate and Transport in the Global Atmosphere*; Pirrone, N., Mason, R.P., Eds.; Springer: New York, NY, USA, 2009; pp. 427–457.
7. Cole, A.S.; Steffen, A. Trends in long-term gaseous mercury observations in the Arctic and effects of temperature and other atmospheric conditions. *Atmos. Chem. Phys.* **2010**, *10*, 4661–4672.
8. Kellerhals, M.; Beauchamp, S.; Belzer, W.; Blanchard, P.; Froude, F.; Harvey, B.; McDonald, K.; Pilote, M.; Poissant, L.; Puckett, K.; *et al.* Temporal and spatial variability of total gaseous mercury in Canada: Results from the Canadian Atmospheric Mercury Measurement Network (CAMNet). *Atmos. Environ.* **2003**, *37*, 1003–1011.
9. Temme, C.; Blanchard, P.; Steffen, A.; Beauchamp, S.T.; Poissant, L.; Tordon, R.J.; Weins, B. Trend, seasonal and multivariate analysis study of total gaseous mercury data from the Canadian Atmospheric Mercury Measurement Network (CAMNet). *Atmos. Environ.* **2007**, *41*, 5423–5441.
10. Poissant, L.; Pilote, M.; Beauvais, C.; Constant, P.; Zhang, H.H. A year of continuous measurements of three atmospheric mercury species (GEM, RGM and Hg_p) in southern Quebec, Canada. *Atmos. Environ.* **2005**, *39*, 1275–1287.
11. Blanchard, P.; Froude, F.A.; Martin, J.B.; Dryfhout-Clark, H.; Woods, J.T. Four years of continuous total gaseous mercury (TGM) measurements at sites in Ontario, Canada. *Atmos. Environ.* **2002**, *36*, 3735–3743.
12. Kim, K.-H.; Ebinghaus, R.; Schroeder, W.H.; Blanchard, P.; Kock, H.H.; Steffen, A.; Froude, F.A.; Kim, M.-Y.; Hong, S.; Kim, J.-H. Atmospheric mercury concentrations from several observatory sites in the Northern Hemisphere. *J. Atmos. Chem.* **2005**, *50*, 1–24.

13. Steffen, A.; Schroeder, W.H.; Macdonald, R.; Poissant, L.; Konoplev, A. Mercury in the Arctic atmosphere: an analysis of eight years of measurements of GEM at Alert (Canada) and a comparison with observations at Amderma (Russia) and Kuujjuarapik (Canada). *Sci. Total Environ.* **2005**, *342*, 185–198.
14. Xu, X.; Akhtar, U.S. Identification of potential regional sources of atmospheric total gaseous mercury in Windsor, Ontario, Canada using hybrid receptor modeling. *Atmos. Chem. Phys.* **2010**, *10*, 7073–7083.
15. Sanei, H.; Outridge, P.M.; Goodarzi, F.; Wang, F.; Armstrong, D.; Warren, K.; Fishback, L. Wet deposition mercury fluxes in the Canadian sub-Arctic and southern Alberta, measured using an automated precipitation collector adapted to cold regions. *Atmos. Environ.* **2010**, *44*, 1672–1681.
16. Prestbo, E.M.; Gay, D.A. Wet deposition of mercury in the U.S. and Canada, 1996–2005: Results and analysis of the NADP mercury deposition network (MDN). *Atmos. Environ.* **2009**, *43*, 4223–4233.
17. Mazur, M.; Mintz, R.; Lapalme, M.; Wiens, B.J. Ambient air total gaseous mercury concentrations in the vicinity of coal-fired power plants in Alberta, Canada. *Sci. Total Environ.* **2009**, *408*, 373–381.
18. Gay, D.A.; Schmeltz, D.; Prestbo, E.; Olson, M.L.; Sharac, T.; Tordon, R. The Atmospheric Mercury Network: measurement and initial examination of an ongoing atmospheric mercury record across North America. *Atmos. Chem. Phys.* **2013**, *13*, 11339–11349.
19. Eckley, C.S.; Parsons, M.T.; Mintz, R.; Lapalme, M.; Mazur, M.; Tordon, R.; Elleman, R.; Graydon, J.A.; Blanchard, P.; St Louis, V.L. Impact of closing Canada's largest point-source of mercury emissions on local atmospheric mercury concentrations. *Environ. Sci. Technol.* **2013**, *47*, 10339–10348.
20. Kirk, J.L.; St. Louis, V.L.; Sharp, M.J. Rapid reduction and reemission of mercury deposited into snow packs during atmospheric mercury depletion events at Churchill, Manitoba, Canada. *Environ. Sci. Technol.* **2006**, *40*, 7590–7596.
21. Stupple, G.W.; Branfireun, B.A. Canopy mercury accumulation in urban and rural forests in southern Ontario. *Environ. Pollut.* **2014**, in preparation.
22. Steffen, A.; Bottenheim, J.; Cole, A.; Ebinghaus, R.; Lawson, G.; Leaitch, W.R. Atmospheric mercury speciation and mercury in snow over time at Alert, Canada. *Atmos. Chem. Phys.* **2014**, *14*, 2219–2231.
23. Steffen, A.; Cole, A.S.; Ariya, P.; Banic, C.; Dastoor, A.; Durnford, D.; Eckley, C.; Graydon, J.A.; Mintz, R.; Pilote, M.; *et al.* Chapter 4: Atmospheric processes, transport, levels and trends. In C*anadian Mercury Science Assessment*; Environment Canada: Toronto, ON, Canada, 2014; in press.
24. Slemr, F.; Brunke, E.; Ebinghaus, R.; Temme, C.; Munthe, J.; Wängberg, I.; Schroeder, W.H.; Steffen, A.; Berg, T. Worldwide trend of atmospheric mercury since 1977. *Geophys. Res. Lett.* **2003**, *30*, 23–21.
25. Slemr, F.; Brunke, E.G.; Ebinghaus, R.; Kuss, J. Worldwide trend of atmospheric mercury since 1995. *Atmos. Chem. Phys.* **2011**, *11*, 4779–4787.
26. Cole, A.; Steffen, A.; Aspmo Pfaffhuber, K.; Berg, T.; Pilote, M.; Tordon, R.; Hung, H. Ten-year trends of atmospheric mercury in the high Arctic compared to Canadian sub-Arctic and mid-latitude sites. *Atmos. Chem. Phys.* **2013**, *13*, 1535–1545.

27. Steffen, A.; Douglas, T.; Amyot, M.; Ariya, P.; Aspmo, K.; Berg, T.; Bottenheim, J.; Brooks, S.; Cobbett, F.D.; Dastoor, A.; *et al.* A synthesis of atmospheric mercury depletion event chemistry in the atmosphere and snow. *Atmos. Chem. Phys.* **2008**, *8*, 1445–1482.
28. Durnford, D.; Dastoor, A.; Ryzhkov, A.; Poissant, L.; Pilote, M.; Figueras-Nieto, D. How relevant is the deposition of mercury onto snowpacks?—Part 2: A modeling study. *Atmos. Chem. Phys.* **2012**, *12*, 9251–9274.
29. Fisher, J.A.; Jacob, D.J.; Soerensen, A.L.; Amos, H.M.; Steffen, A.; Sunderland, E.M. Riverine source of Arctic Ocean mercury inferred from atmospheric observations. *Nat. Geosci.* **2012**, *5*, 499–504.
30. Hirdman, D.; Aspmo, K.; Burkhart, J.F.; Eckhardt, S.; Sodemann, H.; Stohl, A. Transport of mercury in the Arctic atmosphere: Evidence for a springtime net sink and summer-time source. *Geophys. Res. Lett.* **2009,** doi:10.1029/2009GL038345.
31. Lalonde, J.D.; Poulain, A.J.; Amyot, M. The role of mercury redox reactions in snow on snow-to-air mercury transfer. *Environ. Sci. Technol.* **2002**, *36*, 174–178.
32. Lindberg, S.E.; Brooks, S.; Lin, C.-J.; Scott, K.J.; Landis, M.S.; Stevens, R.K.; Goodsite, M.; Richter, A. Dynamic oxidation of gaseous mercury in the Arctic troposphere at polar sunrise. *Environ. Sci. Technol.* **2002**, *36*, 1245–1256.
33. Huang, J.; Miller, M.B.; Weiss-Penzias, P.; Gustin, M.S. Comparison of gaseous oxidized Hg measured by KCl-coated denuders, and nylon and cation exchange membranes. *Environ. Sci. Technol.* **2013**, *47*, 7307–7316.
34. Lyman, S.N.; Jaffe, D.A.; Gustin, M.S. Release of mercury halides from KCl denuders in the presence of ozone. *Atmos. Chem. Phys.* **2010**, *10*, 8197–8204.
35. Graydon, J.A.; St. Louis, V.; Hintlemann, H.; Lindberg, S.E.; Sandilands, K.A.; Rudd, J.W.M.; Kelly, C.A.; Hall, B.; Mowat, L.D. Long-term wet and dry deposition of total and methyl mercury in the remote boreal ecoregion of Canada. *Environ. Sci. Technol.* **2008**, *42*, 8345–8351.
36. Poulain, A.J.; Garcia, E.; Amyot, J.D.; Campbell, P.G.C.; Raofie, F.; Ariya, P.A. Biological and chemical redox transformations of mercury in fresh and salt waters of the high Arctic during spring and summer. *Environ. Sci. Technol.* **2007**, *41*, 1883–1888.
37. Poulain, A.J.; Lalonde, J.D.; Amyot, J.D.; Shead, J.A.; Raofie, F.; Ariya, P.A. Redox transformations of mercury in an Arctic snowpack at springtime. *Atmos. Environ.* **2004**, *38*, 6763–6774.
38. Poissant, L.; Casimir, A. Water-air and soil-air exchange rate of total gaseous mercury measured at background sites. *Atmos. Environ.* **1998**, *32*, 883–893.
39. Choi, H.-D.; Holsen, T.M.; Hopke, P.K. Atmospheric mercury (Hg) in the Adirondacks: Concentrations and sources. *Environ. Sci. Technol.* **2008**, *42*, 5644–5653.
40. Nair, U.S.; Wu, Y.; Walters, J.; Jansen, J.; Edgerton, E.S. Diurnal and seasonal variation of mercury species at coastal-suburban, urban, and rural sites in the southeastern United States. *Atmos. Environ.* **2012**, *47*, 499–508.
41. Poissant, L. Total gaseous mercury in Quebec (Canada) in 1998. *Sci. Total Environ.* **2000**, *259*, 191–201.
42. Liu, B.; Keeler, G.J.; Dvonch, J.T.; Barres, J.A.; Lynam, M.M.; Markis, F.J.; Morgan, J.T. Temporal variability of mercury speciation in urban air. *Atmos. Environ.* **2007**, *41*, 1911–1923.

43. Engle, M.A.; Tate, M.T.; Krabbenhoft, D.P.; Schauer, J.J.; Kolker, A.; Shanley, J.B.; Bothner, M.H. Comparison of atmospheric mercury speciation and deposition at nine sites across central and eastern North America. *J. Geophys. Res.: Atmos.* **2010**, doi:10.1029/2010JD014064.
44. Engle, M.A.; Tate, M.T.; Krabbenhoft, D.P.; Kolker, A.; Olson, M.L.; Edgerton, E.S.; DeWild, J.F.; McPherson, A.K. Characterization and cycling of atmospheric mercury along the central US Gulf Coast. *Appl. Geochem.* **2008**, *23*, 419–437.
45. Fain, X.; Obrist, D.; Hallar, A.G.; McCubbin, I.; Rahn, T. High levels of reactive gaseous mercury observed at a high elevation research laboratory in the Rocky Mountains. *Atmos. Chem. Phys.* **2009**, *9*, 8049–8060.
46. Swartzendruber, P.C.; Jaffe, D.A.; Prestbo, E.; Weiss-Penzias, P.; Selin, N.E.; Park, R.; Jacob, D.J.; Strode, S.; Jaegle, L. Observations of reactive gaseous mercury in the free troposphere at the Mount Bachelor Observatory. *J. Geophys. Res.: Atmos.* **2006**, doi:10.1029/2006JD007415.
47. Poissant, L.; Pilote, M.; Xu, X.; Zhang, H.; Beauvais, C. Atmospheric mercury speciation and deposition in the Bay St. Francois wetlands. *J. Geophys. Res.: Atmos.* **2004**, doi:10.1029/2006JD007415.
48. Bottenheim, J.; Chan, H.M. A trajectory study into the origin of spring time Arctic boundary layer ozone depletion. *J. Geophys. Res.: Atmos.* **2006**, doi:10.1029/2006JD007055.
49. Weiss-Penzias, P.; Gustin, M.S.; Lyman, S.N. Observations of speciated atmospheric mercury at three sites in Nevada: Evidence for a free tropospheric source of reactive gaseous mercury. *J. Geophys. Res.: Atmos.* **2009**, doi:10.1029/2008JD011607.
50. Iverfeldt, A. Occurrence and turnover of atmospheric mercury over the Nordic countries. *Water Air Soil Pollut.* **1991**, *56*, 251–265.
51. Kock, H.H.; Bieber, E.; Ebinghaus, R.; Spain, T.G.; Thees, B. Comparison of long-term trends and seasonal variations of atmospheric mercury concentrations at the two European coastal monitoring stations Mace Head, Ireland, and Zingst, Germany. *Atmos. Environ.* **2005**, *39*, 7549–7556.
52. Slemr, F.; Schell, H.E. Trends in atmospheric mercury concentrations at the summit of the Wank Mountain, southern Germany. *Atmos. Environ.* **1998**, *32*, 845–853.
53. Corbett-Hains, H.; Walters, N.E.; Van Heyst, B.J. Evaluating the effects of sub-zero temperature cycling on mercury flux from soils. *Atmos. Environ.* **2012**, *63*, 102–108.
54. Briggs, C.; Gustin, M.S. Building upon the conceptual model for soil mercury flux: Evidence of a link between moisture evaporation and Hg evasion. *Water Air Soil Pollut.* **2013**, *224*, 1–13.
55. Gustin, M.S.; Stamenkovic, J. Effect of watering and soil moisture on mercury emissions from soils. *Biogeochemistry* **2005**, *76*, 215–232.
56. Lin, C.J.; Gustin, M.S.; Singhasuk, P.; Eckley, C.; Miller, M. Empirical models for estimating mercury flux from soils. *Environ. Sci. Technol.* **2010**, *44*, 8522–8528.
57. Song, X.; Van Heyst, B. Volatilization of mercury from soils in response to simulated precipitation. *Atmos. Environ.* **2005**, *39*, 7494–7505.
58. Zhang, L.; Wright, L.P.; Blanchard, P. A review of current knowledge concerning dry deposition of atmospheric mercury. *Atmos. Environ.* **2009**, *43*, 5853–5864.
59. Baker, K.R.; Bash, J.O. Regional scale photochemical model evaluation of total mercury wet deposition and speciated ambient mercury. *Atmos. Environ.* **2012**, *49*, 151–162.

60. Amos, H.M.; Jacob, D.J.; Holmes, C.D.; Fisher, J.D.; Wang, Q.; Corbitt, E.S.; Galarneau, E.; Rutter, A.P.; Gustin, M.S.; Steffen, A.; *et al.* Gas-particle partitioning of atmospheric Hg(II) and its effect on global mercury deposition. *Atmos. Chem. Phys.* **2012**, *12*, 591–603.
61. Fain, X.; Ferrari, C.P.; Dommergue, A.; Albert, M.R.; Battle, M.; Severinhaus, J.; Arnaud, L.; Barnola, J.-M.; Cairns, W.; Barbante, C.; *et al.* Polar firn air reveals large-scale impact of anthropogenic mercury emissions during the 1970s. *Proc. Natl. Acad. Sci. USA* **2009**, *106*, 16114–16119.
62. Zhang, Y.; Jaeglé, L. Decreases in mercury wet deposition over the United States during 2004–2010: Roles of domestic and global background emission reductions. *Atmosphere* **2013**, *4*, 113–131.
63. Ebinghaus, R.; Jennings, S.G.; Kock, H.H.; Derwant, R.G.; Manning, A.J.; Spain, T.G. Decreasing trends in total gaseous mercury in baseline air at Mace Head, Ireland from 1996–2009. *Atmos. Environ.* **2011**, *159*, 1577–1583.
64. Durnford, D.; Dastoor, A.; Figueras-Nieto, D.; Ryjkov, A. Long range transport of mercury to the Arctic and across Canada. *Atmos. Chem. Phys.* **2010**, *10*, 6063–6086.
65. Strode, S.A.; Jaegle, L.; Jaffe, D.A.; Swartzendruber, P.C.; Selin, N.E.; Holmes, C.D.; Yantosca, R.M. Trans-Pacific transport of mercury. *J. Geophys. Res.: Atmos.* **2008**, doi:10.1029/2007JD009428.
66. Streets, D.G.; Devane, M.K.; Lu, Z.; Sunderland, E.M.; Jacob, D.J. All-time releases of mercury to the atmosphere from human activities. *Environ. Sci. Technol.* **2011**, *45*, 10485–10491.
67. Li, C.; Cornett, J.; Willie, S.; Lam, J. Mercury in Arctic air: The long-term trend. *Sci. Total Environ.* **2009**, *407*, 2756–2759.
68. Soerensen, A.L.; Jacob, D.J.; Streets, D.G.; Witt, M.L.I.; Ebinghaus, R.; Mason, R.P.; Andersson, M.; Sunderland, E.M. Multi-decadal decline of mercury in the North Atlantic atmosphere explained by changing subsurface seawater concentrations. *Geophys. Res. Lett.* **2012**, doi:10.1029/2012GL053736.
69. Poissant, L. Field observation of total gaseous mercury behaviour: Interactions with ozone concentration and water vapour mixing ratio in air at a rural site. *Water Air Soil Pollut.* **1997**, *97*, 341–353.
70. Steffen, A.; Scherz, T.; Olson, M.L.; Gay, D.A.; Blanchard, P. A comparison of data quality control protocols for atmospheric mercury speciation measurements *J. Environ. Monit.* **2012**, *14*, 752–765.
71. Slemr, F.; Ebinghaus, R.; Brenninkmeijer, M.; Hermann, M.; Kock, H.H.; Martinsson, B.G.; Schuck, T.; Sprung, D.; Van Velthoven, P.; Zahn, A.; *et al.* Gaseous mercury distribution in the upper troposphere and lower stratosphere observed onboard the CARIBIC passenger aircraft. *Atmos. Chem. Phys.* **2009**, *9*, 1957–1969.
72. Temme, C.; Einax, J.W.; Ebinghaus, R.; Schroeder, W.H. Measurements of atmospheric mercury species at a coastal site in the Antarctic and over the South Atlantic Ocean during polar summer. *Environ. Sci. Technol.* **2003**, *37*, 22–31.
73. Landis, M.; Stevens, R.K.; Schaedlich, F.; Prestbo, E.M. Development and characterization of an annular denuder methodology for the measurement of divalent inorganic reactive gaseous mercury in ambient air. *Environ. Sci. Technol.* **2002**, *36*, 3000–3009.
74. The Canadian National Atmospheric Chemistry (NAtChem) Database and Analysis System. Available online: http://www.ec.gc.ca/natchem/ (accessed on 29 August 2014).

75. Gilbert, R.O. *Statistical Methods for Environmental Pollution Monitoring*; Van Nostrand Reinhold Company: New York, NY, USA, 1987.
76. van Belle, G.; Hughes, J.P. Nonparametric tests for trend in water quality. *Water Resour. Res.* **1984**, *20*, 127–136.
77. Minamata Convention on Mercury. Available online: http://www.mercuryconvention.org/Convention/tabid/3426/Default.aspx (accessed on 27 June 2014).

© 2014 by the authors; licensee MDPI, Basel, Switzerland. This article is an open access article distributed under the terms and conditions of the Creative Commons Attribution license (http://creativecommons.org/licenses/by/3.0/).